London
Journals Press

IMAGE: OBSERVATORY WITH STAR TRAILS ON MOUNTAINS FOR CLEAR SKY

COMPILED IN UNITED KINGDOM

ENGLISH

They were leaders in building the early foundation of modern programming and unveiled the structure of DNA Their work inspired environmental movements and led to the discovery of new genes They've gone to space and back taught us about the natural world dug up the earth and discovered the origins of our species They broke the sound barrier and gender barriers along the way The world of research wouldn't be the same without the pioneering efforts of famous research works made by these women Be inspired by these explorers and early adopters- the women in research who helped to shape our society We invite you to sit with their stories and enter new areas of understanding This list is by no means a complete record of women to whom we are indebted for their research work but here are of history's greatest research contributions made by...

Read complete here:
https://goo.gl/1vQ3lS

Women In Research

Computing in the cloud!

Cloud Computing is computing as a Service and not just as a Product Under Cloud Computing...

Read complete here:
https://goo.gl/VvHC72

Writing great research...

Prepare yourself before you start Before you start writing your paper or you start reading other...

Read complete here:
https://goo.gl/np73jP

Journal Content
In this Issue

Dr. Saad Subair

College of Computer and Information Sciences, Alazaeim Alazhari University, Khartoum North, Sudan, Associate Professor of Computer Science and Information Ph.D., Computer Science Bioinformatics, University of Technology Malasiya

Gerhard X Ritter

Emeritus Professor, Department of Mathematics, Dept. of Computer & Information, Science & Engineering Ph.D., University of Wisconsin-Madison, USA

Dr. Ikvinderpal Singh

Assistant Professor, P.G. Deptt. of Computer Science & Applications, Trai Shatabdi GGS Khalsa College, India

Prof. Sergey A. Lupin

National Research, University of Electronic Technology Ph.D., National Research University of Electronic Technology, Russia

Dr. Sharif H. Zein

School of Engineering, Faculty of Science and Engineering, University of Hull, UK Ph.D., Chemical Engineering Universiti Sains Malaysia, Malaysia

Prof. Hamdaoui Oualid

University of Annaba, Algeria Ph.D., Environmental Engineering, University of Annaba, University of Savoie, France

Prof. Wen Qin

Department of Mechanical Engineering, Research Associate, University of Saskatchewan, Canada Ph.D., Materials Science, Central South University, China

Luisa Molari

Professor of Structural Mechanics Architecture, University of Bologna, Department of Civil Engineering, Chemical, Environmental and Materials, PhD in Structural Mechanics, University of Bologna.

Prof. Chi-Min Shu

National Yunlin University of Science and Technology, Chinese Taipei Ph.D., Department of Chemical Engineering University of Missouri-Rolla (UMR) USA

Prof. Te-Hua Fang

Department of Mechanical Engineering, National Kaohsiung University of Applied Sciences, Chinese Taipei Ph.D., Department of Mechanical Engineering, National Cheng Kung University, Chinese Taipei

Dr. Fawad Inam

Faculty of Engineering and Environment,
Director of Mechanical Engineering,
Northumbria University, Newcastle upon Tyne,
UK, Ph.D., Queen Mary, University of London,
London, UK

Dr. Rocío Maceiras

Associate Professor for Integrated Science,
Defense University Center, Spain Ph.D., Chemical
Engineering, University of Vigo, SPAIN

Muhammad Hassan Raza

Postdoctoral Fellow, Department of Engineering
Mathematics and Internetworking,
Ph.D. in Internetworking Engineering,
Dalhousie University, Halifax Nova Scotia,
Canada

Rolando Salgado Estrada

Assistant Professor,
Faculty of Engineering, Campus of Veracruz,
Civil Engineering Department, Ph D.,
Degree, University of Minho, Portugal

Abbas Moustafa

Department of Civil Engineering,
Associate Professor, Minia University, Egypt, Ph.D
Earthquake Engineering and Structural Safety,
Indian Institute of Science

Dr. Babar shah

Ph.D., Wireless and Mobile Networks,
Department of Informatics,
Gyeongsang National University,
South Korea

Dr. Wael Salah

Faculty of Engineering,
Multimedia University Jalan Multimedia,
Cyberjaya, Selangor, Malaysia, Ph.D, Electrical and
Electronic Engineering, Power Electronics
and Devices, University Sians Malaysia

Prof. Baoping Cai

Associate Professor,
China University of Petroleum,
Ph.D Mechanical and Electronic Engineering,
China

Prof. Zengchang Qin

Beijing University of Aeronautics
and Astronautics Ph.D.,
University of Bristol,
United Kingdom

Dr. Manolis Vavalis

University of Thessaly,
Associate Professor, Ph.D.,
Numerical Analysis,
University of Thessaloniki, Greece

Dr. Mohammad Reza Shadnam

Canadian Scientific Research and Experimental
Development Manager-Science,
KPMG LLP, Canada, Ph.D., Nanotechnology,
University of Alberta, Canada

Dr. Gang Wang

HeFei University of Technology,
HeFei, China, Ph.D.,
FuDan University, China

Kao-Shing Hwang

Electrical Engineering Dept.,
Nationalsun-Yat-sen University Ph.D.,
Electrical Engineering and Computer Science,
Taiwan

Mu-Chun Su

Electronics Engineering,
National Chiao Tung University, Taiwan,
Ph.D. Degrees in Electrical Engineering,
University of Maryland, College Park

Zoran Gajic

Department of Electrical Engineering,
Rutgers University, New Jersey, USA
Ph.D. Degrees Control Systems,
Rutgers University, United States

Dr. Homero Toral Cruz

Telecommunications,
University of Quintana Roo, Ph.D.,
Telecommunications Center for Research
and Advanced Studies National Polytechnic
Institute, Mexico

Nagy I. Elkalashy

Electrical Engineering Department,
Faculty of Engineering,
Minoufiya University, Egypt

Vitoantonio Bevilacqua

Department of Electrical and Information
Engineering Ph.D., Electrical Engineering
Polytechnic of Bari, Italy

Dr. Sudarshan R. Nelatury

Pennsylvania State University USA Ph.D., Signal
Processing Department of Electronics and
Communications Engineering,
Osmania University, India

Prof. Qingjun Liu

Professor, Zhejiang University, Ph.D.,
Biomedical Engineering,
Zhejiang University, China

Sanjukta Pookulangara

College of Merchandising,
Hospitality and Tourism,
University of North Texas, USA Ph.D, Fashion
Merchandising, University of Missouri Columbia

Prof. Yaohua Zhu

Hong Kong Polytechnic University,
China, PhD. Applied Science and Engineering,
Metallurgy and Materials,
Aston University, UK

Jeng-Da Chai

Associate Professor, Department of Physics,
National Taiwan University,
Excellent Junior Research Investigators,
Ministry of Science and Technology,
Career Development Award,
National Taiwan University

Prof. Peter K. Law

Huazhong University of Science and Technology,
Ph.D., University of Toronto B.Sc.,
McGILL University

Yas Al-Sultani

Ph.D. Image processing Enhancement
using Fuzzy Set Theory Arabian Gulf University,
Constituencies, Training and Continuous
Teaching Center, Iraq

Prof. Dimitrios A. Papaconstantopoulos

School of Physics, Astronomy, and Computational
Sciences, George Mason University, USA
Ph.D., Theoretical Solid State Physics
University of London(UK)

Dr. Abdelkader Zarrouk

Faculty of Sciences, Dept. of Chemistry
Laboratory Applied Chemistry and Environment
Mohammed First University Ph.D.,
Mohammed First Unversity Oujda, Morocco

Prof. Tai-Yin Huang

Associate Professor of Physics, Pennsylvania
State University, Penn State Lehigh Valley,
Ph.D., Physics, University of Cincinnati,
President of the Lehigh Valley,
Taiwanese Women Association

Prof. Dr. Ahmed Asaad Ibrahim Khalil

National Institute for Laser Enhanced Sciences,
NILES Cairo University, Giza, Egypt Ph.D.,
Experimental Physics V Institute
Engineering Application of Lasers
University Bochum, Germany

Dr. Mohamed Salem Badawi

Department of Physics,
Awarded Junior Radiation Physics Medal,
7th Radiation Physics and Protection
Conference, Ismailia, Egypt

Prof. Marie-Christine Record

Department of Chemistry,
Aix-Marseille University Ph.D.,
Materials Sciences, Montpellier University,
France

Prof. Hakan Arslan

Mersin University Ph.D.,
Chemistry Nigde University
Turkey

Prof. Wanyang Dai

Department of Mathematics,
Nanjing University, China
Ph.D., Applied Mathematics,
Georgia Institute of Technology, USA

Dr. Hyongki Lee

Assistant Professor,
University of Houston
Ph.D. in Geodetic Science,
Ohio State University, USA

Nicola Mastronardi

Consiglio Nazionale delle Ricerche,
Ph.D. Applied Mathematics Katholieke
Universiteit Leuven
Belgium

Prof. Saad Belkhiat

Setif University, Ph.D., Physics
University of Sétif
Algeria

Dr. Arvind Chhabra

University of Connecticut Health Center
USA Ph.D., Biotechnology Central
Drug Research Institute

Mohamed Shaaban Ali

Department of Anaesthetics,
Al Salam International Hospital,
The State of Kuwait PhD,
Cerebral Monitoring during cardiac surgery,
University of Wales, Cardiff, UK

Prof. Tarek Aboul-Fadl Mohammad Hassan

Vice Dean for Education and Student Affairs,
Department of Medicinal Chemistry,
Faculty of Pharmacy, Assiut University

Prof. Anthony Bridgwater

European Bioenergy Research Institute,
Director of EBRI, Leader of Aston University
Bioenergy Research Group,
Edwin Walker Prize winner

Prof. Ewa Szczepanska-Sadowska

Medical University of Warsaw,
Poland Ph.D., Medical University of Warsaw,
Poland

Prof. Gjumrakch Aliev

University of Atlanta, Ph.D.,
Cardiovascular Biology and Pathology,
Moscow State University

Prof. Elsayed Ibrahim ELAGAMY

Department of Applied Medical Sciences,
Qassim University, Kingdom of Saudi Arabia,
Ph.D., Dept. of Comparative Medicine,
Mc Gill University

Shen Hu

Division of Oral Biology and Medicine,
Jonsson Comprehensive Cancer Center,
University of California, Ph.D.,
Bioanalytical Chemistry, Wuhan University,
China

Rahul Mahavir Nandre

College of Veterinary Medicine,
Kansas State University, Kansas, USA Ph.D.,
Veterinary Medicine Chonbuk National University,
South Korea

A. C. Matin

Department of Microbiology and Immunology,
Stanford University School of Medicine Stanford,
California Ph.D., Microbiology,
University of California, Los Angeles

Wei Wang

Professor, Public Health School of
Medical Sciences, Ph.D., Edith Cowan University,
Australia

Prof. Filippo Berto

Department of Management and Engineering,
University of Padua, Italy
PH.D, University of Florence

Prof. Bernardino Benito

Department of Accounting and Finance,
Faculty of Economics and Business,
Ph.D. in Economics and Business,
 University of Murcia, SPAIN

Dr. Dimitrios Vortelinos

Department of Accounting,
Economics and Finance, University of Lincoln,
UK Ph.D., Financial Economics,
University of Peloponnese, Greece

Victor J. Tremblay

Department of Economics,
Oregon State University Ph.D.,
Economics Washington State University

Dr. Emmily Mugasia

Department of Education planning and
Management, Masinde Muliro University of Science
and Technology Kakamega – Kenya.

Dr. Randall Xu

School of Business,
Accounting Department University of Houston
-Clear Lake Ph.D. Accounting University of Alabama

Prof. Bartlomiej Kaminski

Information Technology and Management Rzeszow
University Poland Ph.D., Department of Economics
University of Warsaw, Poland

Prof. Ubaldo Comite

University of Calabria,
Arcavacata – Rende,
Italy University Giustino Fortunato,
Benevento – Italy Ph.D.,
Economy and Management
of Public Administrations

Prof. Birendra (Barry) Mishra

Professor of Accounting
A. Gary Anderson Graduate School of Management
University of California, Riverside,
USA Ph.D., Accounting University of Texas, Austin

Xuebing Yang

Assistant Professor,
Economics Penn State Altoona Ph.D.,
University of Oklahoma USA

Prof. Robin H. Luo

Professor of Finance ALHOSN University, UAE
Adjunct DBA Faculty Doctoral Supervisor
University of Liverpool/Laureate, UK Ph.D.,
Nanyang Technological University
Singapore

Omonijo Ojo

Student Industrial Work Experience
Scheme Covenant University, Ota,
Ogun-State Obafemi Awolowo
University Sociology of Development Covenant
University, University Ota, Nigeria

Dr. Haijing Dai

Assistant Professor Chinese University of
Hong Kong Department of Social Work Doctor of
Philosophy Social Work and Sociology University of
Michigan, Ann Arbor

Prof. Yung C. Shin

Purdue University,
USA Ph.D.,
University of Wisconsin, USA

Dr. Xiaochun Cheng

Middlesex University,
UK Ph.D.,
Jilin University China

Prof. Tatiana Kovacikova

COST Office Belgium Ph.D.,
University of Zilina
Slovakia

Dr. José Reinaldo Silva

University of São Paulo Ph.D.,
University of São Paulo
Brazil

Prof. Chang-Hwan Lee

Dong Guk University,
South Korea Ph.D.,
University of Connecticut USA

Prof. Qiuqi Ruan

Beijing Jiaotong University B.S.,
Northern Jiaotong University Beijing

Prof. Victor J. Tremblay

Oregon State University Ph.D.,
Washington State University,
University of California
USA

Prof. Vassili Kolokoltsov

University of Warwick,
UK Ph.D., Moscow State University,
Russia

A Single Server Fuzzy Queue with Reneging and Retention of Reneged Customers

G. Kannadasan & D. Devi

Annamalai University

ABSTRACT

This paper deals with an FM/FM/1 queueing system with reneging and retention of reneged customers and fuzzy parameters. We discuss fuzzy queueintg model and performance measures. We are using α -cuts method in the pentagonal fuzzy numbers. Finally numerical results are presented to show the effects of system parameter.

Keywords: FM/FM/1 queue, Multiple working vacations, Reneging, Retention Membership values pentagonal fuzzy numbers.

Classification: DDC Code: 005.8 LCC Code: QA76.9.A25

Language: English

London Journals Press

London Journal of Research in Science: Natural and Formal

A Single Server Fuzzy Queue with Reneging and Retention of Reneged Customers

G. Kannadasan[α] & D. Devi[σ]

ABSTRACT

This paper deals with an FM/FM/1 queueing system with reneging and retention of reneged customers and fuzzy parameters. We discuss fuzzy queueintg model and performance measures. We are using α - cuts method in the pentagonal fuzzy numbers. Finally numerical results are presented to show the effects of system parameter.

Keywords: FM/FM/1 queue, Multiple working vacations, Reneging, Retention Membership values pentagonal fuzzy numbers.

MSC CODE: 68M20,90B22 6025K

Author α σ : Department of Mathematics, Annamalai University, Annamalainagar-608002, India. Kamban college of arts and science for women, Department of Mathematics, Tiruvannamalai - 606 603.

I. INTRODUCTION

Queueing system with server vacations and impatience of customers have been broadly studied because of their broad applications in day-to-day life congestion problems such as telecommunication systems, service systems and manufacturing systems. Zhang and shi analyzed M/M/1 queue with Bernoulli schedule vacation and vacation interruptions. Selvaraju and Goswami presented impatience customers in single server Markovian queue with single an multiple working vacations. Abou-EI-Ata and Hariri considered multiple servers queueing system M/M/c/N with balking reneging. Kumar and Sharma presented a single server queueing system with retention of reneged customers. Zadeh analyzed membership function which is having more relevance when there is an uncertain situation. Aburba panda and Mahumangalpal presented the pentagonal fuzzy number. Kaufmann introduced an Introduction to the Theory of fuzzy Subsets and Zimmermann explained the Fuzzy Set Theory and Its Applications

In this paper we describe the $FM/FM/1$ queue with reneging and retention of reneged customers.In crisp model,given in section 2.In fuzzy environment and performance of measure, we discuss the fuzzy model with the mean number of customers in the system during working vacation period and normal busy period are studied in fuzzy environment respectively.In section 5 includes numerical study about the performance measures.

London Journal of Research in Science: Natural and Formal

II.   THE CRISP MODEL

We consider an FM/FM/1 queueing model with multiple working vacations, vacations interruptions, reneging, retention of reneged customers an Bernoulli feedback. Customers arrivals to a poisson distribution with parameter λ. The service times during a normal service period η, the service time during a working vacation period η_1 and vacation time σ are according to exponential distribution. During the multiple working vacations the customers are assumed to be impatient, the customer stimulate an impatient timer t_1, which is exponentially distributed with parameter ν. The reneged customer can be retained in the system with probabilitiy δ_1 or the customer abandon the queue with complementary probability $\delta = (1 - \delta_1)$. The server continue a regular busy period with probability β or remains in the vaction with probability $\beta_1 = (1 - \beta)$. After conclusion of each service, the customer can either join the end of the queue with probability ζ or the customer can leave the system with probability γ where $\zeta + \gamma = 1$.

let $M(t)$ denote the number of customer in the system at time t, and let $N(t)$ denote the state of the server at time t with

$$N(t) = \begin{cases} 1 , & \text{if the server is in normal busy busy period} \\ 0 , & \text{if the server is in woring vacation period} \end{cases}$$

Then $\{(M(t), N(t)); t \geq 0\}$ is a continuous time Markov process with state space $\Omega = \{(0,0) \cup (i,j), i = 1,2,3....., j = (0,1)\}$. and steady state condition also satisfied

III.   THE MODEL IN FUZZY ENVIRONMENT

In this section, the arrival rate, service for normal busy period, service for working vacation period, working vacation time, impatients of customers, abandon the queue, leave the system after completion of each service and server resumes a regular busy period are assume to be fuzzy numbers $\bar{\lambda}, \bar{\eta}, \bar{\eta}_1, \bar{\sigma}, \bar{\nu}, \bar{\delta}, \bar{\beta}, \bar{\gamma}$ respectively. Now

$$\bar{\lambda} = \{(x, \mu_{\bar{\lambda}}(x)); x \in S(\bar{\lambda})\},$$

$$\bar{\eta} = \{(y, \mu_{\bar{\eta}}(y)); y \in S(\bar{\eta})\},$$

$$\bar{\eta_1} = \{(y_1, \mu_{\bar{\eta_1}}(y_1)); y_1 \in S(\bar{\eta_1})\},$$

$$\bar{\sigma} = \{(z, \mu_{\bar{\sigma}}(x)); z \in S(\bar{\sigma})\},$$

$$\bar{\nu} = \{(u, \mu_{\bar{\nu}}(u)); u \in S(\bar{\nu})\},$$

$$\bar{\delta} = \{(v, \mu_{\bar{\delta}}(v)); v \in S(\bar{\delta})\},$$

$$\bar{\beta} = \{(r, \mu_{\bar{\beta}}(r)); r \in S(\bar{\beta})\},$$

$$\bar{\gamma} = \{(s, \mu_{\bar{\gamma}}(s)); s \in S(\bar{\gamma})\},$$

where $S(\bar{\lambda})$, $S(\bar{\eta})$, $S(\bar{\eta_1})$, $S(\bar{\sigma})$, $S(\bar{\nu})$, $S(\bar{\delta})$, $S(\bar{\beta})$ and $S(\bar{\gamma})$ are the universal set's of the arrival rate, service for normal busy period, service for working vacation period, working vacation time, impatients of customers, abandon the queue, leave the system after completion of each service and server resumes a regular busy period respectively. Define $f(x, y, y_1, z, u, v, r, s)$ as the system performance measure related to the above defined fuzzy queuing model, which depends on the fuzzy membership function $S(\bar{\lambda})$, $S(\bar{\eta})$, $S(\bar{\eta_1})$, $S(\bar{\sigma})$, $S(\bar{\nu})$, $S(\bar{\delta})$, $S(\bar{\beta})$ and $S(\bar{\gamma})$ Applying Zadeh's extension principle (1978) the membership function of the performance measure $S(\bar{\lambda})$, $S(\bar{\eta})$, $S(\bar{\eta_1})$, $S(\bar{\sigma})$, $S(\bar{\nu})$, $S(\bar{\delta})$, $S(\bar{\beta})$ and $S(\bar{\gamma})$ can be defined as

$$\mu_{\bar{f}(\bar{\lambda},\bar{\eta},\bar{\eta_1},\bar{\sigma},\bar{\nu},\bar{\delta},\bar{\beta},\bar{\gamma})}(H) = \sup_{\substack{x\in S(\bar{\lambda}) \\ y\in S(\bar{\eta}) \\ y_1\in S(\bar{\eta_1}) \\ z\in S(\bar{\sigma}) \\ u\in S(\bar{\nu}) \\ v\in S(\bar{\delta}) \\ r\in S(\bar{\beta}) \\ s\in S(\bar{\gamma})}} \left\{ min \left\{ \mu_{\bar{\lambda}}(x), \mu_{\bar{\eta}}(y), \mu_{\bar{\eta_1}}(y_1), \mu_{\bar{\sigma}}(z), \mu_{\bar{\nu}}(u), \mu_{\bar{\delta}}(v), \mu_{\bar{\beta}}(r), \mu_{\bar{\gamma}}(s) \right\} / H \right\}$$

$$\text{Where} \quad \text{H} = f(x, y, y_1, z, u, v, r, s) \tag{1}$$

If the α- cuts of $f(\lambda, \eta, \eta_1, \sigma, \nu, \delta, \beta, \gamma)$ degenerate to some fixed value, then the system performance is a crisp number, otherwise it is a fuzzy number.

The mean number of customers in the system during working vacation period

$$E[L_1] = \left(\frac{\gamma\eta - \lambda}{\sigma + \beta\gamma\eta_1} \right) - \left[\frac{(\beta\gamma\eta_1)(\sigma + \beta\gamma\eta_1) + (\beta\gamma\eta_1 - (\gamma\eta - \lambda))\eta_1(1 - \beta)\gamma}{(\eta_1(1 - \beta)\gamma)(\sigma + \beta\gamma\eta_1)} \right] A$$

where

$$A = \frac{(1 - \beta)(\delta\nu + \sigma + \beta\gamma\eta_1)(\gamma\eta - \lambda)}{[(1 - \beta)(\delta\nu(\gamma\eta - \lambda) + \gamma(\eta - \eta_1)(\sigma + \gamma\beta\eta_1)) + (\nu\delta\beta + \sigma + \beta\gamma\eta_1)(\sigma + \gamma\beta\eta_1)]}$$

The mean number of customers in the system during normal busy period

$$E[L_2] = \left(\frac{\sigma + \gamma\beta\eta_1}{\gamma\eta - \lambda} \right) \left[\frac{A\lambda - (\delta\nu + \gamma\eta_1 + \sigma - \lambda)B}{\sigma + \gamma\beta\eta_1 + 2\delta\nu} \right]$$

$$+ \left[\frac{(1 - \beta)(\gamma\sigma\eta + \lambda\gamma\beta\eta_1) + [\sigma\beta(\eta_1(1 - \beta)\gamma - (\sigma + \gamma\beta\eta_1)) - (\gamma\sigma\eta + \lambda\gamma\beta\eta_1)]A}{(1 - \beta)(\sigma + \gamma\beta\eta_1)(\gamma\eta - \lambda)} \right]$$

where B=$\left(\dfrac{\gamma\eta - \lambda}{\sigma + \beta\gamma\eta_1}\right) - \left[\dfrac{(\beta\gamma\eta_1)(\sigma + \beta\gamma\eta_1) + (\beta\gamma\eta_1 - (\gamma\eta - \lambda))\eta_1(1 - \beta)\gamma}{(\eta_1(1 - \beta)\gamma)(\sigma + \beta\gamma\eta_1)}\right]A$

we acquire the membership function some performance measures, namely the mean number of customers in the system during working vacation period $E[L_1]$ and the meaan number of customers in the system during normal busy period $E[L_2]$. For the system in terms of this membership function are, as follows

$$\mu_{\overline{[L_1]}}(P) = \sup_{\substack{x \in S(\bar{\lambda}) \\ y \in S(\bar{\eta}) \\ y_1 \in S(\bar{\eta_1}) \\ z \in S(\bar{\sigma}) \\ u \in S(\bar{\nu}) \\ v \in S(\bar{\delta}) \\ r \in S(\bar{\beta}) \\ s \in S(\bar{\gamma})}} \left\{ min \left\{ \mu_{\bar{\lambda}}(x), \mu_{\bar{\eta}}(y), \mu_{\bar{\eta_1}}(y_1), \mu_{\bar{\sigma}}(z), \mu_{\bar{\nu}}(u), \mu_{\bar{\delta}}(v), \mu_{\bar{\beta}}(r), \mu_{\bar{\gamma}}(s) \right\} / P \right\} \quad (2)$$

Where $\quad P = f(x, y, y_1, z, u, v, r, s)$

Where

$$P = \left(\frac{sy - x}{z + rsy_1}\right) - \left[\frac{(rsy_1)(z + rsy_1) + (rsy_1 - (sy - x))y_1(1 - r)s}{(y_1(1 - r)s)(z + rsy_1)}\right]A$$

where

$$A = \frac{(1 - r)(vu + z + rsy_1)(sy - x)}{[(1 - r)(vu(sy - x) + s(y - y_1)(z + sry_1)) + (uvr + z + rsy_1)(z + sry_1)]}$$

$$\mu_{\overline{[L_2]}}(Q) = \sup_{\substack{x \in S(\bar{\lambda}) \\ y \in S(\bar{\eta}) \\ y_1 \in S(\bar{\eta_1}) \\ z \in S(\bar{\sigma}) \\ u \in S(\bar{\nu}) \\ v \in S(\bar{\delta}) \\ r \in S(\bar{\beta}) \\ s \in S(\bar{\gamma})}} \left\{ min \left\{ \mu_{\bar{\lambda}}(x), \mu_{\bar{\eta}}(y), \mu_{\bar{\eta_1}}(y_1), \mu_{\bar{\sigma}}(z), \mu_{\bar{\nu}}(u), \mu_{\bar{\delta}}(v), \mu_{\bar{\beta}}(r), \mu_{\bar{\gamma}}(s) \right\} / Q \right\} \quad (3)$$

Where $\quad Q = f(x, y, y_1, z, u, v, r, s)$

$$Q = \left(\frac{z + sry_1}{sy - x}\right) \left[\frac{Ax - (vu + sy_1 + z - x)B}{z + sry_1 + 2vu}\right]$$

$$+ \left[\frac{(1 - r)(szy + xsry_1) + [zr(y_1(1 - r)s - (z + sry_1)) - (szy + xsry_1)]A}{(1 - r)(z + sry_1)(sy - x)}\right]$$

where B=$\left(\dfrac{sy - x}{z + rsy_1}\right) - \left[\dfrac{(rsy_1)(z + rsy_1) + (rsy_1 - (sy - x))y_1(1 - r)s}{(y_1(1 - r)s)(z + rsy_1)}\right]A$

Using the fuzzy analysis technique describe, we can find the membership of $\mu_{\overline{E[L_1]}}$, $\mu_{\overline{E[L_2]}}$ as a function of the parameter α. Thus the α-cut approach can be used to develop the membership function of $\mu_{\overline{E[L_1]}}$, $\mu_{\overline{E[L_2]}}$.

IV. PERFORMANCE OF MEASURE

The following performance measure are studied for this model in fuzzy environment.

The mean number of customers in the system during working vacation period

Based on Zadeh's extension principle $\mu_{\overline{E[L_1]}}(P)$ is the superimum of minimum over $\mu_{\bar{\lambda}}(x), \mu_{\bar{\eta}}(y), \mu_{\bar{\eta}_1}(y_1), \mu_{\bar{\sigma}}(z), \mu_{\bar{\nu}}(u), \mu_{\bar{\delta}}(v), \mu_{\bar{\beta}}(r), \mu_{\bar{\gamma}}(s)$

$$P = \left(\frac{sy - x}{z + rsy_1} \right) - \left[\frac{(rsy_1)(z + rsy_1) + (rsy_1 - (sy - x))y_1(1 - r)s}{(y_1(1 - r)s)(z + rsy_1)} \right] A$$

to satisfying $\mu_{\overline{E[L_1]}}(P) = \alpha,\ 0 < \alpha \leq 1$.

We consider the following four cases:

case(i);$\mu_{\bar{\lambda}}(x) = \alpha, \mu_{\bar{\eta}}(y) \geq \alpha, \mu_{\bar{\eta}_1}(y_1) \geq \alpha, \mu_{\bar{\sigma}}(z) \geq \alpha, \mu_{\bar{\nu}}(u) \geq \alpha, \mu_{\bar{\delta}}(v) \geq \alpha, \mu_{\bar{\beta}}(r) \geq \alpha, \mu_{\bar{\gamma}}(s) \geq \alpha$

case(ii);$\mu_{\bar{\lambda}}(x) \geq \alpha, \mu_{\bar{\eta}}(y) = \alpha, \mu_{\bar{\eta}_1}(y_1) \geq \alpha, \mu_{\bar{\sigma}}(z) \geq \alpha, \mu_{\bar{\nu}}(u) \geq \alpha, \mu_{\bar{\delta}}(v) \geq \alpha, \mu_{\bar{\beta}}(r) \geq \alpha, \mu_{\bar{\gamma}}(s) \geq \alpha$

case(iii);$\mu_{\bar{\lambda}}(x) \geq \alpha, \mu_{\bar{\eta}}(y) \geq \alpha, \mu_{\bar{\eta}_1}(y_1) = \alpha, \mu_{\bar{\sigma}}(z) \geq \alpha, \mu_{\bar{\nu}}(u) \geq \alpha, \mu_{\bar{\delta}}(v) \geq \alpha, \mu_{\bar{\beta}}(r) \geq \alpha, \mu_{\bar{\gamma}}(s) \geq \alpha$

case(iv);$\mu_{\bar{\lambda}}(x) \geq \alpha, \mu_{\bar{\eta}}(y) \geq \alpha, \mu_{\bar{\eta}_1}(y_1) \geq \alpha, \mu_{\bar{\sigma}}(z) = \alpha, \mu_{\bar{\nu}}(u) \geq \alpha, \mu_{\bar{\delta}}(v) \geq \alpha, \mu_{\bar{\beta}}(r) \geq \alpha, \mu_{\bar{\gamma}}(s) \geq \alpha$

case(v);$\mu_{\bar{\lambda}}(x) \geq \alpha, \mu_{\bar{\eta}}(y) \geq \alpha, \mu_{\bar{\eta}_1}(y_1) \geq \alpha, \mu_{\bar{\sigma}}(z) \geq \alpha, \mu_{\bar{\nu}}(u) = \alpha, \mu_{\bar{\delta}}(v) \geq \alpha, \mu_{\bar{\beta}}(r) \geq \alpha, \mu_{\bar{\gamma}}(s) \geq \alpha$

case(vi);$\mu_{\bar{\lambda}}(x) \geq \alpha, \mu_{\bar{\eta}}(y) \geq \alpha, \mu_{\bar{\eta}_1}(y_1) \geq \alpha, \mu_{\bar{\sigma}}(z) \geq \alpha, \mu_{\bar{\nu}}(u) \geq \alpha, \mu_{\bar{\delta}}(v) = \alpha, \mu_{\bar{\beta}}(r) \geq \alpha, \mu_{\bar{\gamma}}(s) \geq \alpha$

case(vii);$\mu_{\bar{\lambda}}(x) \geq \alpha, \mu_{\bar{\eta}}(y) \geq \alpha, \mu_{\bar{\eta}_1}(y_1) \geq \alpha, \mu_{\bar{\sigma}}(z) \geq \alpha, \mu_{\bar{\nu}}(u) \geq \alpha, \mu_{\bar{\delta}}(v) \geq \alpha, \mu_{\bar{\beta}}(r) = \alpha, \mu_{\bar{\gamma}}(s) \geq \alpha$

case(vii);$\mu_{\bar{\lambda}}(x) \geq \alpha, \mu_{\bar{\eta}}(y) \geq \alpha, \mu_{\bar{\eta}_1}(y_1) \geq \alpha, \mu_{\bar{\sigma}}(z) \geq \alpha, \mu_{\bar{\nu}}(u) \geq \alpha, \mu_{\bar{\delta}}(v) \geq \alpha, \mu_{\bar{\beta}}(r) \geq \alpha, \mu_{\bar{\gamma}}(s) = \alpha$

For case (i) the lower and upper bound of α- cuts of $\mu_{\overline{E[L_1]}}$ can be acquire through the corresponding parametric non-linear programs,

$$[E[L_1]]_{\alpha}^{L_1} = \min_{\Omega} \{[P]\} \text{ and}$$

$$[E[L_1]]_{\alpha}^{U_1} = \max_{\Omega} \{[P]\}$$

Similarly, we can calculate the lower and upper bounds of the α-cuts of $[E[L_1]]$ for the case $(ii), (iii), (iv)(v), (vi)$ and (vii). By considering all the cases simultaneously the lower and upper bounds of the α-cuts of $[E[L_1]]$ can be written as

$$P = \left(\frac{sy - x}{z + rsy_1} \right) - \left[\frac{(rsy_1)(z + rsy_1) + (rsy_1 - (sy - x))y_1(1 - r)s}{(y_1(1 - r)s)(z + rsy_1)} \right] A$$

$$[E[L_1]]_\alpha^L = \min_\Omega \{[P]\} \quad \text{and} \quad [E[L_1]]_\alpha^U = \max_\Omega \{[P]\}.$$

such that

$$x_\alpha^L \le \mathrm{x} \le x_\alpha^U, \ y_\alpha^L \le y \le y_\alpha^U, \ y_{1\alpha}^L \le y_1 \le y_{1\alpha}^U, \ z_\alpha^L \le z \le z_\alpha^U,$$

$$u_\alpha^L \le u \le u_\alpha^U, v_\alpha^L \le v \le v_\alpha^U, r_\alpha^L \le r \le r_\alpha^U, s_\alpha^L \le s \le s_\alpha^U .$$

If both $[E[L_1]]_\alpha^L$ and $[E[L_1]]_\alpha^U$ are invertible with respect to α, the left and right shape function, $L(M) = [E[L_1]_\alpha^L]^{-1}$ and $R(M) = [E[L_1]_\alpha^L]^{-1}$ can be derived from which the membership function $\mu_{\overline{E[L_1]}}(M)$ can be constructed as

$$\mu_{\overline{E[L_1]}}(P) = \begin{cases} L(P), & [E[L_1]]_{\alpha=0}^L \le P \le [E[L_1]]_{\alpha=0}^U \\ 1, & [E[L_1]]_{\alpha=1}^L \le P \le [E[L_1]]_{\alpha=1}^U \\ R(P), & [E[L_1]]_{\alpha=1}^L \le P \le [E[L_1]]_{\alpha=0}^U \end{cases} \tag{4}$$

In the same way we get the following results.

The mean number of customersin the system during normal busy period

$$\mu_{\overline{E[L_2]}}(Q) = \begin{cases} L(Q), & E[L_2]_{\alpha=0}^L \le Q \le E[L_2]_{\alpha=0}^U \\ 1, & E[L_2]_{\alpha=1}^L \le Q \le E[L_2]_{\alpha=1}^U \\ R(Q), & E[L_2]_{\alpha=1}^L \le Q \le E[L_2]_{\alpha=0}^U \end{cases} \tag{5}$$

V.   NUMERICAL STUDY

The mean number of customers in the system during working vacation period
Suppose the fuzzy arrival rate $\overline{\lambda}$, service rate for normal busy period $\overline{\eta}$, service rate for working vacation period $\overline{\eta_1}$, working vacation time $\overline{\sigma}$,impatients of customers $\overline{\nu}$, abandon the queue $\overline{\delta}$, leave the system after completion of each service $\overline{\beta}$, server resumes a reular busy period $\overline{\gamma}$, are assumed to be pentagonal fuzzy numbers described by:
$\overline{\lambda} = [1,2,3,4,5]$, $\overline{\eta} = [6,7,8,9,10]$, $\overline{\eta_1} = [11,12,13,14,15]$ $\overline{\sigma} = [21,22,23,24,25]$,
$\overline{\nu} = [31,32,33,34,35]$, $\overline{\delta} = [26,27,28,29,30]$, $\overline{\beta} = [41,42,43,44,45]$, $\overline{\gamma} = [36,37,8,39,40]$
 per hour respectively then

$$\lambda(\alpha) = \min_{x \in s(\overline{\lambda})} \{x \in s(\overline{\lambda}), G(x) \ge \alpha\}, \max_{x \in s(\overline{\lambda})} \{x \in s(\overline{\lambda}), G(x) \ge \alpha\},$$

where

$$
G(x) = \begin{cases} 0 & ,if \ \ x \leq a_1 \\ 1 - (1-r)\dfrac{x - a_2}{a_3 - a_2} & ,if \ a_2 \leq \ x \leq a_3 \\ 1 \ if \ x = a_3 \\ 1 - (1-r)\dfrac{a_4 - x}{a_4 - a_3} & ,if \ a_3 \leq \ x \leq a_4 \\ r\dfrac{a_5 - x}{a_5 - a_4} & ,if \ a_4 \leq \ x \leq a_5 \\ 0 & ,if \ x \geq a_5 \end{cases}
$$

That is, $\lambda(\alpha) = [1 + \alpha, 5 - \alpha]$, $\eta(\alpha) = [6 + \alpha, 10 - \alpha]$, $\eta_1(\alpha) = [11 + \alpha, 15 - \alpha]$, $\sigma(\alpha) = [21 + \alpha, 25 - \alpha]$, $\nu(\alpha) = [31 + \alpha, 35 - \alpha]$, $\delta(\alpha) = [26 + \alpha, 30 - \alpha]$, $\beta(\alpha) = [41 + \alpha, 45 - \alpha]$, $\gamma(\alpha) = [36 + \alpha, 40 - \alpha]$

It is clear that, when $x = x_\alpha^U$, $y = y_\alpha^U$, $y_1 = (y_1)_\alpha^U$, $z = z_\alpha^U$, $u = u_\alpha^U$, $v = v_\alpha^U$, $r = r_\alpha^U$ and $s = s_\alpha^U$ P attains its maximum value and when $x = x_\alpha^L$, $y = y_\alpha^L$, $y_1 = (y_1)_\alpha^L$, $z = z_\alpha^U$, $u = u_\alpha^L$, $v = v_\alpha^V$, $r = r_\alpha^L$ and $s = s_\alpha^L$ P attains its minimum value.

From the generated for the given input values of $\overline{\lambda}, \ \overline{\eta}, \overline{\eta}_1, \ \overline{\sigma}, \ \overline{\nu}, \ \overline{\delta}, \ \overline{\beta} \ \overline{\gamma}$,

i) For fixed values of x, y, y_1, z, u, v and r, P decreases as s increase.

ii) For fixed values of y, y_1, z, u, v, r and s, P decreases as x increase.

iii) For fixed values of y_1, z, u, v, r, s and x, P decreases as y increase.

iv) For fixed values of z , u, v, r, s, x and y, P decreases as y_1 increase.

v) For fixed values of u, v, r, s, x, y and y_1, P decreases as z increase.

vi) For fixed values of v, r, s, x, y, y_1 and z, P decreases as u increase.

vii) For fixed values of r, s, x, y, y_1, z and u, P decreases as v increase.

viii) For fixed values of s, x, y, y_1, z, u and v, P decreases as r increase.

The smallest value of occurs when x-takes its lower bound. i.e)., $x = 16 + \alpha$ and y, y_1, z, u, v, r and s take their upper bounds given by $y = 10 - \alpha$, $y_1 = 15 - \alpha$, $z = 25 - \alpha$, $u = 35 - \alpha$, $v = 30 - \alpha$, $r = 45 - \alpha$ and $s = 40 - \alpha$ respectively. And maximum value of $E[L_1]$ occurs when $x = 5 - \alpha$, $y = 6 + \alpha$, $y_1 = 11 + \alpha$, $z = 21 + \alpha$, $u = 31 + \alpha$, $v = 26 + \alpha$, $r = 41 + \alpha$, and $s = 36 + \alpha$. If both $[E[L_1]]_\alpha^L$ & $[E[L_1]]_\alpha^U$ are invertible with respect to $'\alpha'$ then, the left shape function $L(P) = [E[L_1]_\alpha^L]^{-1}$ and right shape function $R(P) = [E[L_1]_\alpha^U]^{-1}$ can be acquired and from which the membership function $\mu_{\overline{E[L_1]}}(P)$ can be constructed as:

$$
\mu_{\overline{E[L_1]}}(P) = \begin{cases} 0, & if \ \ P \leq P_1 \\ 0.4(x - 2), & if \ P_1 \leq P \leq P_2, \\ 0.4(4 - x), & if \ P_2 \leq P \leq P_3, \\ 0.6(5 - x), & if \ P_3 \leq P \leq P_4, \\ 0, & if \ P \leq P_5 \end{cases} \tag{6}
$$

The values of P_1, P_2, P_3, P_4 and P_5 as acquired from (8) are:

$$\mu_{\overline{E[L_1]}}(P) = \begin{cases} 0, & if \ P \leq 0.0000 \\ 0.4(x-2), & if \ 0.0000 \leq P \leq 0.01223, \\ 1, & if \ x = 1 \\ 0.4(4-x), & if \ 0.01223 \leq P \leq 0.05788, \\ 0.6(5-x), & if \ 0.05788 \leq P \leq 0.02245, \\ 0, & if \ P \geq 0.0000 \end{cases}$$

In the same way we get the following results.

The mean number of customersin the system during normal busy period

$$\mu_{\overline{E[L_2]}}(Q) = \begin{cases} 0, & if \ \ Q \leq Q_1 \\ 0.5(x-2), & if \ Q_1 \leq Q \leq Q_2, \\ 0.5(4-x), & if \ Q_2 \leq Q \leq Q_3, \\ 0.5(5-x), & if \ q_3 \leq Q \leq Q_4, \\ 0, & if \ Q \geq Q_5 \end{cases} \tag{7}$$

The values of Q_1, Q_2, Q_3, Q_4 and Q_5 as acquired from (9) are:

$$\mu_{\overline{E[L_2]}}(Q) = \begin{cases} 0, & if \ Q \leq 0.0000 \\ 0.5(x-2), & if \ 0.0000 \leq Q \leq 0.6331, \\ 0.5(4-x), & if \ 0.6331 \leq Q \leq 1.1266, \\ 0.5(5-x), & if \ 1.1266 \leq Q \leq 0.8810, \\ 0, & if \ Q \geq 0.0000 \end{cases}$$

VI.   CONCLUSION

In this paper we have studied the analysis of $M/M/1$ queue with reneging and retention of reneged customers using pentagonal fuzzy numbers. we have obtained the performance measure such as the mean number of customers in the system during working vacation period,the mean number of customers in the system during normal busy period. we have obtained the numerical result to all the performance measures for this fuzzy queues. In this queueing model is very important in system performance and solve various problems in many complex system,such as communication systems,computer systems,call centers and flexible manfacturing systems.

REFERENCES

1. Zhang,H.;Shi,.:The M/M/1 queue with Bernoulli schedule-controlle vacation and vacation interruption.Int.J.Inf.
2. Selvaraj,N.;Goswami,c.: Impatient customers in an M/M/1 queue with single and mltiple working vacations. Comput.Ind.Eng. 65 (2), 207-215 (2013)
3. Abou El-Ata,M.O.;Hariri, A.M.A.: The M/M/c/N queue with balking and reneing. Compuut. Oper. Res. 19 (13), 713-716.
4. Kumar, R.; Sharma,S.H.:M/M/1/N queueing system withretention of renege customers. Pak. J. Stat. Oper. Res. 8,859-866(2012).
5. Zadeh, L.A.: 1965 fuzzy set information and control 8338-353.
6. Apurba panda,.; Madhumangal Pal.: 2015 A stuy on pentagonal fuzzynmber and its corresponding matrices Paci_c Sciences Review B: Humanities and Social Sciences 1 131-139
7. Kaufmann,A.: 1975, Introduction to the Theory of fuzzy Subsets, Vol.1.Academic Press, New York.
8. Zimmermann, H.J.: 2001, Fuzzy Set Theory and Its Applications, Kluwer Academic, Boston.

This page is intentionally left blank

Phytochemical Screening, GC-MS and Histological Effects of Methanolic Leaf Extract of *Hippocratea Africana* (Willd) on the Midgut of *Sitophilus zeamais* (Motsch)

Diligent Efiong Oboho, Akwaowo Uduehe Nelson, Affiong Edeke, Jude Ifeanyichukwu Okwor, Cyril Ali Imakwu, Akaninyene Udoh Akpan, Samson Oyebadejo & Joseph Effiong Eyo

ABSTRACT

Phytochemicals in methanolic leaf extract of *Hippocratea africana* using qualitative and Gas Chromatography-Mass Spectrum (GC-MS) analysis to determine the phytochemicals present and its effect on the histology of midgut of *Sitophilus zeamais*. Insects were administered with 10mg/kg of the plant extract using diffusion method where insects were put in a petri dish containing various concentrations and observed to see the stage they begin to die due to toxicity and observed for 5 minutes. They were collected into foil processing paper and fixed in Bouins fluid for 24 hours, repacked after 24 hours and folded in fresh foil immersed in buffered formalin for histopathological studies. Result revealed that a severe degeneration de-arrangement of the respiratory tract epithelial lining, secretory lining cells and gastrointestinal layers with the destruction of the muscular layer when compared with the control. The methanol leaf extracts of *H. africana* were preliminary screened for the phytochemicals. The extract shows the presence of cardiac glycosides, saponin, steroids/terpenes, flavonoids, alkaloids and phenols.

Keywords: GC-MS, *Hippocratea africana,* Histology, Phytochemistry**,** *Sitophilus zeamais.*

Classification: DDC Code: 333.793   LCC Code: HD9502.5.M472

Language: English

Phytochemical Screening, GC-MS and Histological Effects of Methanolic Leaf Extract of *Hippocratea Africana* (Willd) on the Midgut of *Sitophilus zeamais* (Motsch)

Diligent Efiong Oboho[α], Akwaowo Uduehe Nelson[σ], Affiong Edeke[ρ], Jude Ifeanyichukwu Okwor[ᴄᴅ] Cyril Ali Imakwu[¥], Akaninyene Udoh Akpan[§], Samson Oyebadejo[Χ] & Joseph Effiong Eyo[ᵛ]

ABSTRACT

Phytochemicals in methanolic leaf extract of *Hippocratea africana* using qualitative and Gas Chromatography-Mass Spectrum (GC-MS) analysis to determine the phytochemicals present and its effect on the histology of midgut of *Sitophilus zeamais*. Insects were administered with 10mg/kg of the plant extract using diffusion method where insects were put in a petri dish containing various concentrations and observed to see the stage they begin to die due to toxicity and observed for 5 minutes. They were collected into foil processing paper and fixed in Bouins fluid for 24 hours, repacked after 24 hours and folded in fresh foil immersed in buffered formalin for histopathological studies. Result revealed that a severe degeneration de-arrangement of the respiratory tract epithelial lining, secretory lining cells and gastrointestinal layers with the destruction of the muscular layer when compared with the control. The methanol leaf extracts of *H. africana* were preliminary screened for the phytochemicals. The extract shows the presence of cardiac glycosides, saponin, steroids/terpenes, flavonoids, alkaloids and phenols. GC-MS analysis of the extract showed the presence of showed eight major compounds as shown on Table 4. They were: 5-amino-1- tetrazolylacetic acid [RT-83.55017, Peak Percentage- 1.173%], 2-amino-4-(2-methylpropenyl) -pyrimidin-5 carboxylic acid [RT- 83. 978, Peak Percentage 1.713%], Cedrandiol [RT-87.201, Peak Percentage-2.445%, Malic acid [RT 88. 740, Peak Percentage 1.431%], 1, 2 benzenedimethanethiol [RT-91.634, PeakPercentage - 2.045%], ethyl 5- (furan-2-yl)-1, 2-oxazole-3-carboxylate [RT-89.693, Peak erce-ntage-1.446%], Mephenesin [RT-92.587, Peak Percentage-1.911%]. The findings indicated that methanol extract of *H. africana* is rich in phyto-compounds having biological activities on the midguts' histology of *S. zeamais*. Therefore, it is recommended as an alternative for the synthetic insecticide used by farmers for the preservation of stored grains.

Keywords: GC-MS, *Hippocratea africana,* Histology, Phytochemistry*, Sitophilus zeamais.*

I. INTRODUCTION

Despite encouraging efforts over the past 2-3 decades to isolate botanicals with enhanced insecticidal potential for insect management as an alternative to synthetic insecticides, there is still inadequate information available in terms of their synergistic potential, toxicology, optimum use and species specificity (1, 2). Many botanicals are used by small scale farmers as insecticides in both homes and subsistence farming. Certain of the compounds derived from plants are screened and marketed as insecticides. Since plant materials are rich in phytochemicals, their extracts and secondary metabolite have been used to control insect pests of various orders (3, 4, 5).

Hippocratea africana (Willd.) Loes.ex Engl. (Celastraceae) syn. *Loeseneriella africana* (Willd.) N.Hallé is a perennial, hairless (glabrous) green forest climber, reproducing from seeds (Figure 1), (6). It is commonly referred to as 'African paddle-pod.' The Nigerian tribe 'Efik' and 'Ibibio' call it "Eba enang enang" while Oro people

calls it 'Mkpak oyo'ananang'. Tropical Africa is home to this plant. The Efik and Ibibios Niger Delta region in Nigeria have long utilized the root of this plant to treat different maladies such as fever, convulsions, malaria, bodily discomfort, diabetes, and diarrhea (7). Decoction of the plant's root is also employed as an antidote or antipoison for the treatment of liver and inflammatory illnesses such as jaundice and hepatitis, according to an ethnobotanical survey (8, 9). The root was found to have anti-plasmodial activity (6), anti-inflammatory and analgesic (10), anti-diarrheal, antiulcerative (11), anti-diabetic and hypolipidemic (12, 13). Other biological activities that have been express by this plant include: beta-cell cytotoxicity, anti-oxidant burst and anti-leishmanial, hepatoprotective activity (14), anticonvulsant and antibacterial activities (15). Plants have evolved a variety of defense mechanisms to reduce insect attack, both constitutive and inducible, however, there are few investigation on the application of plant as a natural insecticide. Hence, this study reports the phytochemical constituents of *Hippocratea africana* using Gas Chromatography- Mass spectroscopy and determine the effect of the extracts on the histology of insect midgut.

Figure 1: Hippocratea africana (Dalziel, 1956)

II.   MATERIAL AND METHODS

2.1 Collections and Identification of Plant Materials

Fresh leaves of *Hippocratea africana* (Figure 1) were obtained from Faculty of Pharmacy Medicinal Farm of University of Uyo, Akwa Ibom State and authenticated by a taxonomist in the Department of Botany and Ecological Studies, University of Uyo. Voucher specimens with number: UUH/3689 was deposited in their herbarium for further referencing.

2.2 Rearing of Test Organisms

Sitophilus zeamais cultures were established to provide equivalent age weevils for the experiment. A total of ten (10 kg) bean seeds were obtained and cleaned to remove any seeds that had evident damage. To prevent field infestation, the clean seeds were kept in a sealed container in the refrigerator at 4°C for a month. Seeds were placed in plastic bags and stored at room temperature for two weeks. *S. zeamais* were taken from contaminated bean grains and their sexes were established by inspecting their snouts. Females have a longer and thinner snout, while males have a shorter and fatter snout. In addition, females have smooth textured bodies, whilst males have rough textured bodies (16). The insects were cultivated in jars holding 100 weevils per 400 g of seeds that had been cleaned and sterilized. To allow aeration and prevent weevil escape, the jar was covered with muslin cloth and held in place with a rubber band at room temperature. All parent weevils in each jar were removed seven days after oviposition (17). To distinguish the sexes, the dimorphic rostral features were used (18, 19, 20, 21). The jars were kept in an insect rearing cage at the University of Uyo's Entomology Laboratory, Department of Animal and Environmental Biology. The experiment used two day-old newly emerging insects.

2.3 Preparation of plant powder and extract

After collection, the plant leaves were washed and chopped into pieces and room dried to a constant weight. Using an electric blender (Braum Multiquick Immersion, B White Mixer MR 5550CA, Germany), the dried leaves were grinded and fine powder was then kept in an airtight container for further analysis. The bioactive components in the leaves were extracted using methanol according to the reported standard procedures (21, 22. 23). Briefly, 50 g of the powder was soaked for 48 – 72 hours at room temperature in 95 % methanol. The crude extract

Phytochemical Screening, GC-MS and Histological Effects of Methanolic Leaf Extract of Hippocratea Africana (Willd) on the Midgut of Sitophilus Zeamais (Motsch)

12 Volume 22 | Issue 4 | Compilation 1.0   © 2022 London Journals Press

were then filtered using rotary evaporator, then stored in the refrigerator for use.

2.4 Phytochemical Analysis of the Plants

The preliminary phytochemical screening of the plant was carried out in Pharmacognosy Laboratory of University of Uyo, Akwa Ibom State using the standard procedures as described by (24, 25, 26, 27).

2.5 Gas Chromatography- Mass Spectroscopy Analysis

A GC Clarus 500 Perkin Elmer system and gas chromatograph were interfaced with a mass detector (Turbo mass gold Perkin Elmer) (GC-MS) according to (28, 29). Column: Elite-5MS (5 percent diphenyl/95 percent dimethyl poly siloxane), 30 x 0.25 mm x 0 25m df, Carrier gas: Helium (99.999 percent) with constant flow rate of 1 mL per min, (Split ratio: 10:1), Sample Injection volume 2 l, Software: Turbo mass 5.2, Oven operating in electron impact mode at 70eV, oven temperature was fixed from 110°C (isothermal The injector was set to 250°C, the ion source to 280°C, and the total GC run time was 36 minutes. The GC- MS was conducted in Multi- User Science Research Laboratory, Department of Chemistry, Ahmadu Bello University (ABU) Zaria Kaduna Nigeria.

2.6 Histopathological Assay of Insects

Using the method of Humason (32), insects were administered with 10g the plant extract and observed for 5 minutes using diffusion method where insects were put in a petri dish containing various concentrations and observed to see the stage they begin to die due to toxicity. They were collected into foil processing paper and fixed in Bouins fluid for 24 hours, repacked after 24 hours and folded in fresh foil immersed in buffered formalin for histopathological studies. After 48 hours of fixations, samples were labeled according to the groups and process to paraffin wax by passing the basket of insects through 10 % formal saline for 2 hours. 1 hour in 3 changes of alcohol for dehydration ranging from 70% to 100%, 2 changes of xylene for clearing, 2 changes of melted paraffin wax at 56°C for impregnation for 2 hours, samples were embedded in melted paraffin wax to create support for the tissues in the embedding cassettes. Then microtomy was carried out using Rotary Microtome by sectioning the embedded tissues at 5 um and mounted the cut sections in ribbons from water bath on the labeled glass slide, drained of excess water, allowed to dry using hot plate and stained with hematoxylin and Eosin technique by dewaxing with xylene, taking the section to water, by passing through descending grade of alcohol, stained for nuclear content in hematoxylin for 10 minutes, washed in water, differentiate in 1% acid alcohol and blue in saturated solution of lithium carbonate solution, washed in water and counter stained briefly in eosin, for 3 minutes, then section were washed briefly and dehydrated, cleared in xylene, mounted with DPX, cover-slipped and observed under digital microscope for pathological changes.

III. RESULTS

To investigate the importance of any medicinal plant, the initial or first step is to screen for its phytochemicals, as it gives a broad knowledge with respect to the nature of the compounds present in it. In the present study, the methanol leaf extracts of *H. africana* were preliminary screened for the phytochemicals. The extract shows the presence of cardiac glycosides, saponin, steroids/terpenes, flavonoids, alkaloids and phenols as shown in Table 1.

Phytochemical Screening, GC-MS and Histological Effects of Methanolic Leaf Extract of Hippocratea Africana (Willd) on the Midgut of Sitophilus Zeamais (Motsch)

© 2022 London Journals Press

Volume 22 | Issue 4 | Compilation 1.0

13

London Journal of Research in Science: Natural and Formal

Table 1: Qualitative phytochemical analysis of the different extracts

	H. africana	Test
Anthraqunones	-	Borntrager
Steroids/terpenes	+++	Liebermann-Burchard
Cardiac glycoside	++	Keller-kiliani, Salkowsiki
Saponin	++	Frothing, Fehling solution, Na_2Co_3
Tannins and Phenols	++	Ferric Chloride, Pb acetate
Flavonoids	+++	NaOH, Mayer, Wagner
Alkaloids	++	NaOH, Shinda
Phlobatannins	++	Dragendoff, Mayer, Wagner

+++= Strongly present; ++ = moderately present; += trace; - = absent + = present

The results of the qualitative phytochemicals revealed the presence of different metabolites and their intensity was determined based on colours as shown in Table 1a. Flavonoids, Steroids and terpenes were stongly present in *H. africana*. Anthraquinones were absent in *H. africana*. Cardiac glycosides, Tannins and Phenols, alkaloids, phlobatannins and saponin were moderately present.

GC-MS: The compound name, molecular formulae, molecular weight, peak area and retention time of the bioactive compounds were ascertained. The relative percentage amount of each component was calculated by comparing its average peak area to the total mass. The result of Gas Chromatography-Mass Spectroscopy of the extracts of *U. chamae* are as shown on Table 2.The extracts of *U. chamae* showed eight (8) major compounds: Thiirane [RT-40.712, Peak Percentage 1.539%], 1,1, dimethylhydrazine [RT-41.115, Peak Percentage-1.861%], malic acid [RT- 91.304, Peak Percentage- 2.040%], 2-amino-4-(2-methylpropenyl)-pyrimidin-5-carboxylic acid [RT-84.846, Peak Percentage-1.554%], L-aspartic acid [RT-85.846, Peak Percentage- 2.001%], 2- nitro benzaldehyde [RT-86.505, Peak Percentage- 3.903%], Cedrandiol [RT-87.055, Peak Percentage- 1.751%] and Mercaptoethanol [RT- 88.300, Peak Percentage- 1.115%]. The phytochemicals from the extract are known to control insects by eroding the cuticle layer and causing dehydration. These phytochemicals are known to block the spiracles of insect and causing death by asphyxiation hence, the insecticidal efficacy of the plant.

Histologic section of the *S. zeamais* treated with concentrated *Hippocratea africana* and treatment at magnification X400 revealed severe de-arrangement of the respiratory, secretory and gastrol intestinal layer with destruction of the muscular layer when compared to the control group.

Phytochemical Screening, GC-MS and Histological Effects of Methanolic Leaf Extract of Hippocratea Africana (Willd) on the Midgut of Sitophilus Zeamais (Motsch)

14 Volume 22 | Issue 4 | Compilation 1.0 © 2022 London Journals Press

Table 2: Chemical Composition of Methanol Extract of *H. africana*

S/N	Compound	RT	Area (%)	Chemical Formula	Molecular Weight	Structure
1	5-amino-1-tetrazolylacetic acid	83.55017	1.173	$C_2H_3N_5O_2$	129.08	
2	2-amino-4-(2-methylpropenyl)-pyrimidin-5-carboxylic acid	83.978	1.713	$C_9H_{11}N_3O_2$	193.20	
3	Cedrandiol	87.201	2.445	$C_{15}H_{26}O_2$	238.37	
4	Malic acid	88.740	1.431	$C_5H_8O_4$	132.11	
5	1,2-benzenedimethanethiol	91.634	2.045	$C_8H_{10}S_2$	170.29	
6	Ethyl 5-(furan-2-yl)-1,2-oxazole-3-carboxylate	89.693	1.446	$C_{10}H_9NO_4$	207.18	
7	2-amino-4-(2-methylpropenyl)-pyrimidin-5-carboxylic acid	89.949	1.868	$C_9H_{11}N_3O_2$	193.20	
8	Mephenesin	92.587	1.911	$C_{10}H_{14}O_3$	182.22	

Phytochemical Screening, GC-MS and Histological Effects of Methanolic Leaf Extract of Hippocratea Africana (Willd) on the Midgut of Sitophilus Zeamais (Motsch)

© 2022 London Journals Press

Volume 22 | Issue 4 | Compilation 1.0

15
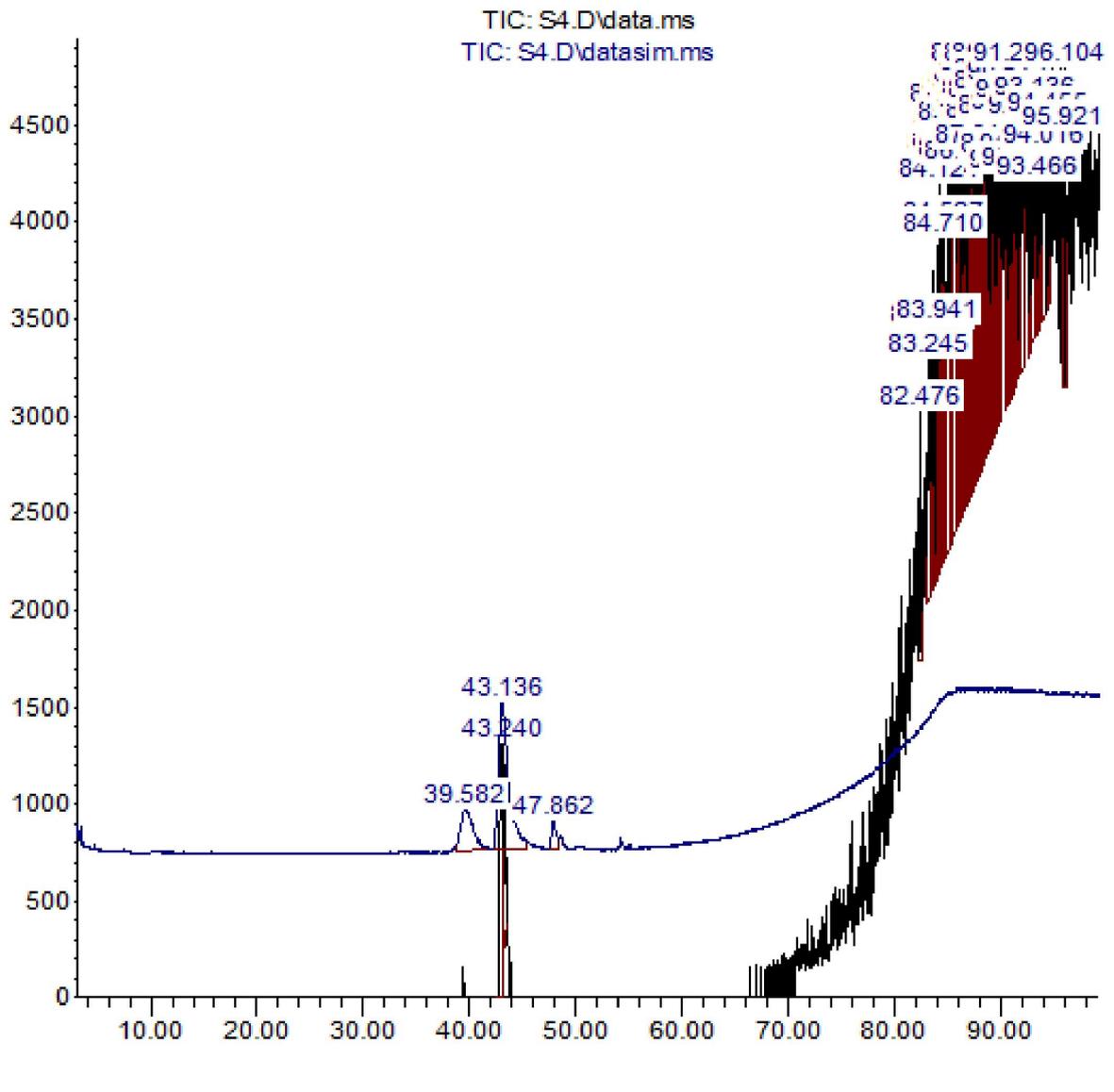
Figure 2: GC-MS of methanol leaf extract of Hippocratea africana

Phytochemical Screening, GC-MS and Histological Effects of Methanolic Leaf Extract of Hippocratea Africana (Willd) on the Midgut of Sitophilus Zeamais (Motsch)

16   Volume 22 | Issue 4 | Compilation 1.0   © 2022 London Journals Press
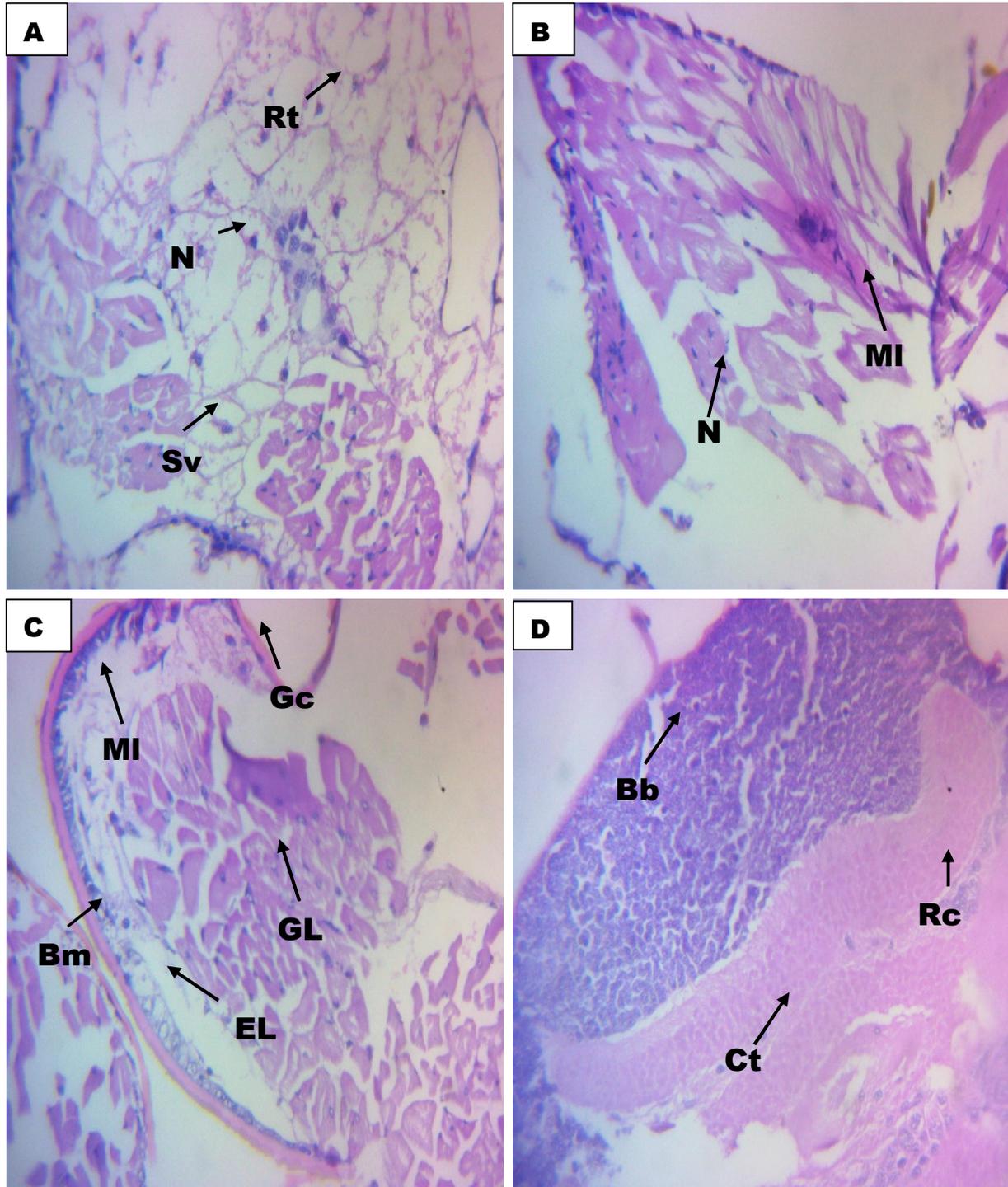
Photomicrographs of Weevils without treatment at magnification x400 stained with H&E method

Keys: Epithelium Lining (**EL**), Basement membrane (**BM**), Regenerative Cells (**Rc**), Gut Lumen (**GL**), Muscular Layer (**ML**), Secretory Vesicles (**SV**), Goblet cells (**Gc**), Connective Tissue (**Ct**) Respiratory tract (**Rt**) and Nucleus (**N**)
A= Respiratory Tract, **B**= Muscle, **C**=Gastro-intestinal Tract and **D**= Excretory system

London Journal of Research in Science: Natural and Formal

Phytochemical Screening, GC-MS and Histological Effects of Methanolic Leaf Extract of Hippocratea Africana (Willd) on the Midgut of Sitophilus Zeamais (Motsch)

© 2022 London Journals Press

Volume 22 | Issue 4 | Compilation 1.0

17
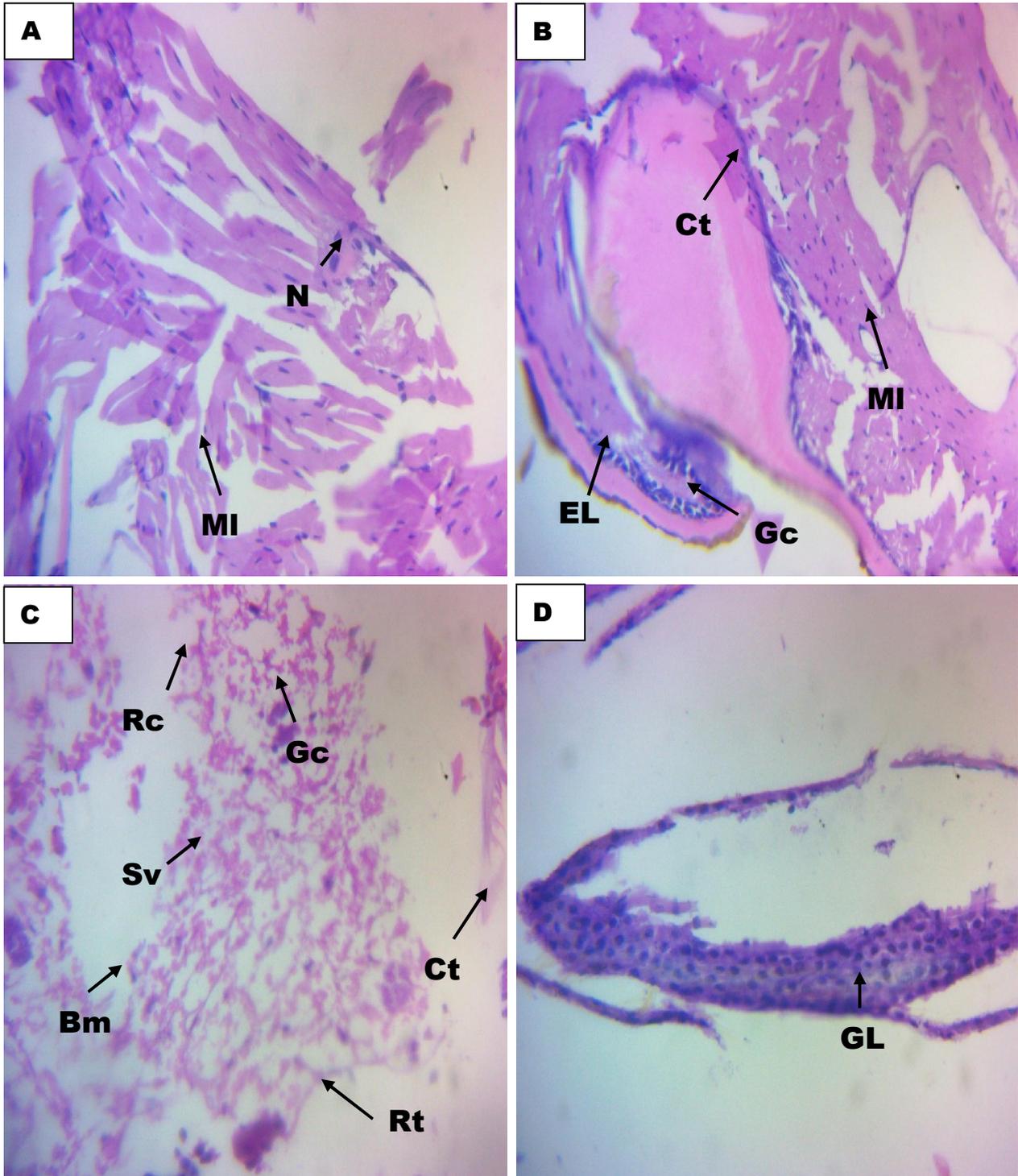
Photomicrographs of maize weevils treated with 10mg/kg of *H. africana* at magnification x400 stained with H&E method

Keys: Epithelium Lining (**EL**), Basement membrane (**BM**),Brush Boader(**Bb**), Regenerative Cells (**Rc**), Gut Lumen (**GL**), Muscular Layer (**ML**), Secretory Vesicles (**SV**), Goblet cells (**Gc**) Connective Tissue (**Ct**) Respiratory tract(**Rt**) and Nucleus (**N**)
A= Respiratory Tract, **B**= Muscle, **C**=Gastro-intestinal Tract and **D**=   Excretory system

London Journal of Research in Science: Natural and Formal

Phytochemical Screening, GC-MS and Histological Effects of Methanolic Leaf Extract of Hippocratea Africana (Willd) on the Midgut of Sitophilus Zeamais (Motsch)

18   Volume 22 | Issue 4 | Compilation 1.0   © 2022 London Journals Press

IV. DISCUSSION

Anthraquinone was not present in this study while Phlobotannins was moderately present. This work is consistent with the findings of (33,34,35) who carried out the phytochemical screening of extract of *L. africana and H. africana* and reported no trace of anthraquinone and moderately presence of Phlobatannins. The heavy presence of cardiac glycosides found in this study is consistent with the results of (33,34) who observed heavy presence of the same metabolites when carrying out the phytochemical screening of *L. africana and H. africana* but disagrees with the findings of (36) who did not detect any trace of cardiac glycosides when screening the extract of *H. africana.* It agrees with Mikali *et al.* (37) who observed similar phytoconstituents from methanolic leaf extract of *Ficus exasperate.*

There was great destruction of the mid-gut cells. The results was also in agreement with the findings of (38) who investigated the histological changes in the midgut of the larvae of *Agrotis ipsilon* treated with methoprene. The effect of the different treatment on the midgut epithelium was the exfoliation from the basemen membrane and partial destruction of cell lining. Meanwhile epithelial lining was strongly vacuolated and considerably elongated, lines in between cells disappear and the peritrophic membrane was moderately destroyed. The findings were consistent with those of (39) who found histopathological abnormalities, nuclei dissolving, and epithelial cell degeneration in two-day-old *Rynchophorus ferrugineus* larvae poisoned by two biopesticides, Boxus chinensis oil and precocene II. After two days of treatment with seven Essential oils (EO) concentrations, (40) discovered anomalies in the mid-gut and developing oocytes of female *Trogoderma granarium* treated as 4th instar larvae. The findings are likewise consistent with those of (41) who found significant effects on the alimentary canal and fat bodies of *H. littoralis* 1st nymphal instars after treatment with sub-lethal quantities of three oils from garlic, mint, and Eucalyptus. Epithelial cells were destroyed, microvilli were curled and ruptured, and the peritrophic membrane was curled and ruptured, compared to the control group. In the present investigation, the peritrophic membrane, striated border, secretory cells, and regeneration cells in the treated mid-gut sections of weevils with extract were significantly disrupted as compared to the control. This was in agreement with (42) who observed expansion of epithelial cells, development of vacuoles at the apical region of the cell, and breakdown of the peritrophic membrane in *Culex pipiens* larvae after exposure to chamomile oil extract. It also backed up the findings of (43) who found the same effect when *Datura alba* leaf extract was tested on the midgut of *Periplaneta americana.* Ranjini and Nambiar (44) also observed an elongated columnar cells, vacuolization of cytoplasm, increased goblet cells and thinning of the muscle layers when tested the effect of leaf extracts of *Clerodendrum infortunatum* and *Eupatorium odoratum* on the mid-gut tissue of sixth instar larvae of *Orthaga exvinacea.* The results also agreed with (45) who observed hypertrophy and lysis of epithelium intestinal cells when extract of *Ricinus communis* leaves were tested on the larvae of mosquito, *Culex pipiens.* The study therefore, identified *S. zeamais* economic role as a serious threat to maize production in Nigeria. Because the plant used to control the weevil is safe for animals at the dosages reported, more effort should be put into cultivating, packing, and using it as a botanical pesticide on a broad scale.

V. CONCLUSION

The disproportionate use of synthetic pesticides results in the secondary outbreak and rapid proliferation of the pests usually under natural control. The environmental concerns have become an inevitable part of human livelihood over the last few decades. As a result, an important quest of the day has become the hunt for safer and environmentally friendly implements for both agricultural and medical uses.

REFERENCES

1. Ferede Negasi, S. Studies on the Economic Importance and Control of Bean Bruchids in Haricot Bean. MSc. Thesis, 1994. Alemaya University, Alemaya, Ethiopia.

Phytochemical Screening, GC-MS and Histological Effects of Methanolic Leaf Extract of Hippocratea Africana (Willd) on the Midgut of Sitophilus Zeamais (Motsch)

© 2022 London Journals Press

Volume 22 | Issue 4 | Compilation 1.0

19

2. Araya, G. and Getu, E. Evaluation of botanical plants powders against Zabrotes subfasciatus (Boheman) (Coleoptera: Bruchidae) in stored haricot beans haricot bean under laboratory condition. African Journal of Agricultural Research, 2009; 4: 1073-1079.

3. Dalziel, J. M. Useful Plants of West Tropical Africa 1956. Crown Agents for Overseas Government, London.

4. Packiam, S. M., Baskar, K. and Ignacimuthu, S. Insecticidal and histopathological effects of botanical formulations against Helicoverpa armigera (Hub.) (Lepidoptera: Noctuidae). Journal of Agricultural Technology, 2013;9 (3): 553-563.

5. George, K., Jayaprakasam, B., Dalavoy, S. S. and Nair, M.G. Pest-managing activities of plant extracts and anthraquinones from Cassia nigricans from Burkina Faso. BioResource Technology, 2008;99: 2037-2045.

6. Muthu, C., Baskar, K., Kingsley, S. and Ignacimuthu, S. Bioefficacy of Clerodendrum phlomidis Linn. F. and Fleuggea leucopyrus (Koen.) Willd. against Earias vitelli Fab. Journal of Entomology, 2013;9:332-342

7. Okokon, J. E., Ita, B. N. and Udokpoh, A. E. The in vivo antimalarial activities of Uvaria chamae and Hippocratea africana. Pathogens and Global Health, 2006; 100(7): 585-90.

8. Etukudo, I. Ethnobotany, Conventional and Traditional Uses of Plants 2003. The Verdict Press, Uyo, Nigeria.

9. Ajibesin, K. K., Ekpo, B. A., Bala, D. N., Essien, E. E. and Adesanya, S. A. Ethnobotanical survey of Akwa Ibom State of Nigeria. Journal of Ethnopharmacology, 2008;115: 387-408.

10. Okokon, J. E., Antia, B. S. and Umoh, E. E. Analgesic and anti-inflammatory activities of Hippocratea africana. International Journal of Pharmacology, 2008; 4(1): 51-55.

11. Okokon, J. E., Akpan, H. D., Ekaidem, I. and Umoh, E. E. Antiulcer and antidiarrhoeal activities of Hippocratea africana. Pakistan Journal of Pharmaceutical Sciences, 2011;24(2): 201-205.

12. Okokon, J. E., Antia, B. S., Umoh, E. E. and Etim, E. I. Antidiabetic and hypolipidaemic activities of Hippocratea africana (Hippocrateaceae) in streptozotocin induced diabetic rats. International Journal of Drug Development and Research, 2010; 2(3): 501-506.

13. Ndem, J. I., Eteng, M. U. and Uwah, A. F. Effects of Hippocratea africana root bark extract on lipid profile of female and male albino wistar rats. Journal of Scientific Research and Reports, 2014;3(19): 2574-2583.

14. Okokon, J. E., Dar, A. and Choudhary, M. I. Cellular antioxidant, cytotoxic and antileishmanial activities of Hippocratea africana. Journal of Nature and Pharmaceuticals, 2013c; 4(2):81-85.

15. Okokon, J. E., Davies, K., Antia, B. S. and Okokon, P. J. Depressant, anticonvulsant and antibacterial activities of Hippocratea africana. International Journal of Phytotherapy, 2014; 4(3): 144-153.

16. Kranz, J., Schmutterer, H. and Koch, W. Diseases, Pests, and Weeds in Tropical Crops, 1977. John Wiley and Sons, Incorporated, Great Britain.

17. Walgenbach, C. A., Phillips, J. K., Faustini, D. L. and Burkholder, W. E. Male-produced aggregation pheromone of the maize weevil, Sitophilus zeamais, and interspecific attraction between three Sitophilus species. Journal of Chemical Ecology, 1983; 9(7): 831-841.

18. Adedire, C. O. Biology, ecology and control of insect pests of stored grains. Pages 59 – 94. In: Ofuya, T. I. and Lale, N. E. S. (Eds). Pest of Stored Cereals and Pulses in Nigeria, 2001. Dave Collins Publications, Akure, Nigeria.

19. Odeyemi, O. O. and Daramola, A. M. Storage Practices in the Tropics: Food Storage and Pest Problems, 2000. Dave Collins Publications, Akure, Nigeria.

20. Halstead, D. G. H. External sex differences in stored-products Coleoptera. Bulletin of Entomological Research, 1963; 54(1): 119-134.

21. Oboho D, S Oyebadejo, I Edagha, P Ubulom, B Ita, A Nelson, A Akpan, J Eyo (2021). Gas Chromatography-Mass Spectroscopy and histopathological effects of methanol leaf extract of *Uvaria chamae* on the midgut of *Sitophilus zeamais. Intl J Agric Biol* 26:695–701

Phytochemical Screening, GC-MS and Histological Effects of Methanolic Leaf Extract of Hippocratea Africana (Willd) on the Midgut of Sitophilus Zeamais (Motsch)

20 Volume 22 | Issue 4 | Compilation 1.0   © 2022 London Journals Press

22. Mukhtar, M. D. and Huda, M. Prevalence of Tinea capitis in primary school and sensitivity of etiological agents of Pisti astratiotes extracts. Nigerian Journal of Microbiology, 2005;19 (1-2): 412-419.

23. Santana, P. M., Miranda, M., Payrol, J. A., Silva, M., Hernandez, V. and Peralta, E. Gas Chromatography- Mass Spectrometry Study from the Leaves Fractions Obtained from Vernonanthura patens (Kunth) H. Rob. International Journal of Organic Chemistry, 2013; 3(2):32968. http://dx.doi.org/10.4236/ijoc.2013.32011

24. Fatope, M. O., Ibrahim, H. and Takeda, Y. Screening of higher plants reputed as pesticides using the brine shrimp lethality assay. International Journal of Pharma-cognosy, 1999; 31(4): 250-254.

25. Prashant, T., Bimlesh, K., Mandeep, K., Gurpreet, K. and Harleen, K. Phytochemical screening and extraction: a review. Internationale Pharmaceutica Sciencia, 2011;1(1): 98-106.

26. Kokate, C. K., Purohit, A. P. and Gokhale, S. B. Pharmacognosy. 40th Edition, 2008. Nirali Prakashan, India.

27. Evans, W. C. Trease and Evans' Pharmacognosy. 15th Edition, Elsevier, 2002. A Division of Reed Elsevier India Pvt. Limited, India.

28. Harborne, J. B. Phytochemical Methods. 2nd Edition, 1984. Chapman and Hall, New York.

29. Mishra, M., Gupta, K. K. and Kumar, S. Impact of the stem extract of Thevetia neriifolia on the feeding potential and histological architecture of the midgut epithelial tissue of early fourth instars of Helicoverpa armigera Hübner. International Journal of Insect Science, 2015; 7: 53-60.

30. Hema, R., Kumaravel, S. and Sivasubramanian, C. GC-MS study on the potentials of Syzygium aromaticum. Rese-archer, 2010; 2(12): 1-4.

31. Ousman, A., Ngassoum, M. B., Essia-Ngang, J. J., Ngamo, L.S.T. and Ndjouvenkwu, R. Insecticidal activity of spicy plant oils against Sitophilus zeamais in stored maize in Cameroun. Agriculture Journal, 2007; 2(2): 192-196.

32. Abbott, W. S. A method of computing the effectiveness of an insecticide. Journal of Economic Entomology, 1925;18: 65 – 66

33. Humason, G. L. Animal Tissue Techniques. 4th Edition, 1979.W.H. Freeman, San Francisco, USA.

34. Ekanem, N. G., Mbagwu, H. O. C. and Harry, G. I. Phytochemical screening and hypogl ycaemic activity of Lasianthera africana Beauv. (Aquifoliales: Stemonuraceae) leaf extract on diabetic rats. Brazilian Journal of Biological Sciences, 2016;3(6): 293-298.

35. Folawewo, A. D., Madu, A. N., Agbaje-Daniels, F. V., Faboyede, A. O. and Coker, A. R. Phytochemical screening and antibacterial activities of the root bark extracts of Hippocratea africana (Willd.) Loes. ex Engl. European Journal of Medicinal Plants, 2017;19(1): 1-8.

36. Ebana, R. U., Asamudo, N. U., Etok, C. A., Edet, U. O. and Onyebuisi, C. S. Phytochemical Screening, Nutrient Analysis and Antimicrobial Activity of the leaves of Lasianthera africana and Dennettia tripetala on Clinical Isolates. Journal of Advances in Biology and Biotechnology, 2016;8(4): 1-9

37. Rajeswari, K., Ravi Kumar, A. and Subbu Rathinam, K. M. Phytochemical and antidiarrhoeal activity of Hippocratea Africana roots. Indian Journal of Research in Pharmacy and Biotechnology, 2014; 2(4): 1357- 1359

38. Mikail, H. G., Akumka, D. D., Adamu, M. and Zaifada, A. U. Evaluation of phytochemical constituents and sedative-hypnotic activity of the methanol leaf extract of Ficus exasperata in mice. Veterinary World, 2019;12(6): 830-833

39. Abdou, L. W. and Abdel-Hakim, A. E. Some biological and biochemical aspects of Agrotis ipsilon (Lepidoptera: Noctuidae) larvae as Influenced by Methoprene (JHA). Current Science International, 2017; 6(3): 631-639.

40. Abdullah, M. A. Toxicological and histop-athological studies of Boxus chinensis oil and precocene II on larvae of the red palm weevil Rynchophorus ferrugineus (Oliver) (Coleoptera: Curculionidae). Egyptian

London Journal of Research in Science: Natural and Formal

Phytochemical Screening, GC-MS and Histological Effects of Methanolic Leaf Extract of Hippocratea Africana (Willd) on the Midgut of Sitophilus Zeamais (Motsch)

© 2022 London Journals Press

Volume 22 | Issue 4 | Compilation 1.0

21

Academic Journal of Biological Sciences. A, Entomology, 2009; 2(2): 45-54.

41. Ahmed, G. A. Biological, Biochemical and Histological Studies on the Effect of Some Botanical Oils on the Khapra Beetle, Trogoderma granarium Everts (Coleoptera: Dermestidae). PhD Thesis, 2010. Department of Zoology, Faculty of Science, Alexandria University, Egypt.

42. Sharaby, A., Montasser, S. A., Mahmoud, Y. A. and Ibrahim, S. A. Natural plant essential oils for controlling the grasshopper (Heteracris littoralis) and their pathological effects on the alimentary canal. Ecologia Balkanica, 2012;4 (1): 39-52.

43. Ahmed, F. A. Safety and Efficiency of Natural and Synthetic Insecticides Used in the Control of Culicine Mosquitoes in Egypt. PhD Thesis, 1995. Faculty of Science, Zagazig University, Egypt.

44. Khan, I., Qamar, A., Mehdi, S. H. and Shahid, M. Histopathological effects of Datura alba leaf extract on the midgut of Periplaneta americana. Biology and Medicine, 2011;3: 260-264.

45. Ranjini, K. R. and Nambiar, J. G. Histopathological effects of leaf extracts of Clerodendrum infortunatum and Eupatorium odoratum on the midgut tissue of sixth instar larvae of Orthaga exvinacea Hampson (Lepidoptera: Pyralidae). Journal of Entomology and Zoology Studies, 2015; 3: 296-301.

46. Aouinty, B., Chennaoui, M., Mahari, S., Rihane, A. and Mellouki, F. Larvicidal effects of aqueous extract from Ricinus communis L. leaves against mosquito Culex pipiens: mortality and histopathology of treated larvae. Journal of Material and Environmental Science, 2018; 9, 619-623.

London Journal of Research in Science: Natural and Formal

Phytochemical Screening, GC-MS and Histological Effects of Methanolic Leaf Extract of Hippocratea Africana (Willd) on the Midgut of Sitophilus Zeamais (Motsch)

22 Volume 22 | Issue 4 | Compilation 1.0

© 2022 London Journals Press

Analysis of Fm/Fg/1 Retrial Queue with Bernoulli Schedule and Vacation using Hexagonal Fuzzy Numbers

G. Kannadasan & V. Padmavathi

Annamalai University

ABSTRACT

We discuss about the deals for "Analysis of FM/FG/1 Retrial Queue with Bernoulli Schedule and acation using Hexagonal Fuzzy Numbers" using fuzzy techniques. This fuzzy queueing model, researches obtains some performance measure of interest such as the mean number of customers in the orbit, the mean number of customers in the system and the mean waiting time in the system. Finally numerical results are pre- sented using hexagonal fuzzy numbers to show the effects of system parameters.

Keywords: M/G/1 model; Membership values; Retrial Queue; Hexagonal fuzzy numbers.

Classification: MSC 11B68, 94D05

Language: English

Analysis of Fm/Fg/1 Retrial Queue with Bernoulli Schedule and Vacation using Hexagonal Fuzzy Numbers

G. Kannadasan[α] & V. Padmavathi[σ]

ABSTRACT

We discuss about the deals for "Analysis of FM/FG/1 Retrial Queue with Bernoulli Schedule and acation using Hexagonal Fuzzy Numbers" using fuzzy techniques. This fuzzy queueing model, researches obtains some performance measure of interest such as the mean number of customers in the orbit, the mean number of customers in the system and the mean waiting time in the system. Finally numerical results are pre- sented using hexagonal fuzzy numbers to show the effects of system parameters.

Keywords: M/G/1 model; Membership values; Retrial Queue; Hexagonal fuzzy numbers.

Author α: Department of Mathematics, Annamalai University, Annamalainagar-608002, India.
σ: Department of Mathematics, Annamalai University, Annamalainagar-608002, India.

I. INTRODUCTION

Queueing systems with repeated attempts are characterized by the fact that a customer finding all the servers busy upon arrival must leave the service area and repeat his request for service after some random time. Between trials, the blocked customer joins a pool of unsatisfied customers called "orbit". Yang and Li[1] has investigated the M/G/1 retrial queue with the server subject to starting failures. Lie and Lee[2] Analysis of fuzzy queues computers an mathematics with applications. Ke et.al[3] studied On retrial queuing model with fuzzy parameter. Negi and Lee[4] investigated and simulation of fuzzy queue fuzzy sets and Systems. Dhurai and Karpagam[5] analyzed a new membership function on hexagonal fuzzy numbers. Zadeh[6] considered Fuzzy sets as a basis a theory of possibility. Rita and Robert[7] studied Application of fuzzy set theory to retrial queues. This paper is organized as follows. In division 2 describe deals the fuzzy queue model. In division 3 we discuss the mean number of customers in the orbit, the mean number of customers in the system and the mean waiting time in the system are studied in fuzzy environment. In division 4 includes numerical study about the performance measures. Finally, conclusion are gained.

II.   THE CRISP MODEL

Consisder an M/G/1 retrial queueing model with Bernoulli schedule and vacation. Customer arrive from outside the system according to a Poisson process with parameter λ. The server provides service rates common distribution with parameter μ_1 and μ_2. The server takes a Bernoulli vacation after each service completion, the server takes a vacation with probability q, and with probability p = 1-q, the vacation rates two moments ξ_1, ξ_2. Arrival rates, service rates, server vacation rates are assumed to be mutually independent.

The state of the system at time t can be described by the Markov process $\{N(t); t > 0\} = \{(C(t), Y(t), \xi_0(t), \xi_1(t), \xi_2(t) \geq 0\}$, where C(t) denotes the server state (0,1 or 2 depending if the server is free, busy or on vacation respectively) and X(t) corresponding to the number of customers in the orbit at time t. If C(t) = 0 and $X(t) > 0$, then $\xi_0(t)$, represents the elapsed retrial time, if C(t) = 1, then $\xi_1(t)$ corresponds to the elapsed time of the customer served, if C(t) = 2 and $Y(t) \geq 0$, then $\xi_2(t)$, represents the elapsed vacation time at time t.

(i) The mean number of customers in the orbit

$$\text{E(O)} = \frac{\lambda^2 p \xi_2}{2[\lambda \xi_1 + 1]} + \frac{\lambda^2 \mu_2 + \lambda^2 q \xi_2 + 2\lambda^2 q \xi_1 \mu_1}{2[1 - \lambda \mu_1 - \lambda q \xi_1]}$$

(ii) The mean number of customers in the system

$$\text{E(S)} = \lambda \mu_1 + \frac{2\lambda^2 \mu_1 \xi_1 + \lambda^2 \xi_2 + \lambda^2 \mu_2}{2[1 - \lambda(\mu_1 + \xi_1)]}$$

(iii) The mean waiting time in the system

$$\text{E(W)} = \mu_1 + \frac{2\lambda \mu_1 \xi_1 + \lambda \xi_2 + \lambda \mu_2}{2[1 - \lambda(\mu_1 + \xi_1)]}$$

III.   THE MODEL IN FUZZY ENVIRONMENT

In this section the arrival rate λ, service rate μ_1, μ_2, vacation rate ξ_1, ξ_2 are assumed to be fuzzy numbers respectively.

Now,
$$\bar{\lambda} = \{(b, \mu_{\bar{\lambda}}(b)); b \in s(\bar{\lambda})\}$$
$$\bar{\mu}_1 = \{(c_1, \mu_{\bar{\mu}_1}(c_1)); c_1 \in s(\bar{\mu}_1)\}$$
$$\bar{\mu}_2 = \{(c_2, \mu_{\bar{\mu}_2}(c_2)); c_2 \in s(\bar{\mu}_2)\}$$
$$\bar{\xi}_1 = \{(d_1, \mu_{\bar{\xi}_1}(d_1)); d_1 \in s(\bar{\xi}_1)\}$$
and
$$\bar{\xi}_2 = \{(d_2, \mu_{\bar{\xi}_2}(d_2)); d_2 \in s(\bar{\xi}_2)\}$$

Where $S(\bar{\lambda})$, $S(\bar{\mu_1})$, $S(\bar{\mu_2})$, $S(\bar{\xi_1})$, $S(\bar{\xi_2})$ are the universal sets of the arrival rate, service rate, vacation rate and reneging respectively. Define $f(b, c_1, c_2, d_1, d_2)$ as the system performance measure related to the above defined fuzzy queueing model, which depends on the fuzzy membership function $f(\bar{\lambda}, \bar{\mu_1}, \bar{\mu_2}, \bar{\xi_1}, \bar{\xi_2})$. Applying Zadeh's extension principle (1978) the membership function of the performance measure $f(\bar{\lambda}, \bar{\mu_1}, \bar{\mu_2}, \bar{\xi_1}, \bar{\xi_2})$ can be defined as

$$\mu_{\bar{f}(\bar{\lambda}, \bar{\mu_1}, \bar{\mu_2}, \bar{\xi_1}, \bar{\xi_2})}(H) = \sup_{\substack{b \in S(\bar{\lambda}) \\ c_1 \in S(\bar{\mu_1}) \\ c_2 \in S(\bar{\mu_2}) \\ d_1 \in S(\bar{\xi_1}) \\ d_2 \in S(\bar{\xi_2})}} \left\{ min \left\{ \mu_{\bar{\lambda}}(b), \mu_{\bar{\mu_1}}(c_1), \mu_{\bar{\mu_2}}(c_2), \mu_{\bar{\xi_1}}(d_1), \mu_{\bar{\xi_2}}(d_2) \right\} / H \right\} \quad (1)$$

where,
$$H = f(b, c_1, c_2, d_1, d_2)$$

If the α- cuts of $f(\bar{\lambda}, \bar{\mu_1}, \bar{\mu_2}, \bar{\xi_1}, \bar{\xi_2})$ degenerate to some fixed value, then the system performance is a crisp number, otherwise it is a fuzzy number.

We obtain the membership function some performance measures namely the mean number of customers in the orbit E(O), the mean number of customers in the system E(S), the mean waiting time in the system E(W). For the system in terms of this membership function are, as follows

$$\mu_{\overline{E[O]}}(I) = \sup_{\substack{b \in S(\bar{\lambda}) \\ c_1 \in S(\bar{\mu_1}) \\ c_2 \in S(\bar{\mu_2}) \\ d_1 \in S(\bar{\xi_1}) \\ d_2 \in S(\bar{\xi_2})}} \left\{ min \left\{ \mu_{\bar{\lambda}}(b), \mu_{\bar{\mu_1}}(c_1), \mu_{\bar{\mu_2}}(c_2), \mu_{\bar{\xi_1}}(d_1), \mu_{\bar{\xi_2}}(d_2) \right\} / I \right\} \quad (2)$$

where,
$$I = f(b, c_1, c_2, d_1, d_2)$$

where,

$$I = \frac{b^2 p d_2}{2[bpd_1 + 1]} + \frac{b^2 c_2 + b^2 q d_2 + 2b^2 q d_1 c_1}{2[1 - bc_1 - bqd_1]}$$

$$\mu_{\overline{E[S]}}(J) = \sup_{\substack{b \in S(\bar{\lambda}) \\ c_1 \in S(\bar{\mu_1}) \\ c_2 \in S(\bar{\mu_2}) \\ d_1 \in S(\bar{\xi_1}) \\ d_2 \in S(\bar{\xi_2})}} \left\{ min \left\{ \mu_{\bar{\lambda}}(b), \mu_{\bar{\mu_1}}(c_1), \mu_{\bar{\mu_2}}(c_2), \mu_{\bar{\xi_1}}(d_1), \mu_{\bar{\xi_2}}(d_2) \right\} / J \right\} \quad (3)$$

where,
$$J = f(b, c_1, c_2, d_1, d_2)$$

where,

$$J = bc_1 + \frac{2b^2 c_1 d_1 + b^2 d_2 + b^2 c_2}{2[1 - b(c_1 + d_1)]}$$

$$\mu_{\overline{E[W]}}(K) = \sup_{\substack{b \in S(\bar{\lambda}) \\ c_1 \in S(\bar{\mu_1}) \\ c_2 \in S(\bar{\mu_2}) \\ d_1 \in S(\bar{\xi_1}) \\ d_2 \in S(\bar{\xi_2})}} \left\{ min \left\{ \mu_{\bar{\lambda}}(b), \mu_{\bar{\mu_1}}(c_1), \mu_{\bar{\mu_2}}(c_2), \mu_{\bar{\xi_1}}(d_1), \mu_{\bar{\xi_2}}(d_2) \right\} / K \right\} \tag{4}$$

where,

$$K = f(b, c_1, c_2, d_1, d_2)$$

where,

$$K = c_1 + \frac{2bc_1 d_1 + bd_2 + bc_2}{2[1 - b(c_1 + d_1)]}$$

Using the fuzzy analysis technique explain, we can find the membership of $\mu_{\overline{E[O]}}$, $\mu_{\overline{E[S]}}$, $\mu_{\overline{E[W]}}$ as a function of the parameter α. Thus the α-cut approach can be used to develop the membership function of $\mu_{\overline{E[O]}}$, $\mu_{\overline{E[S]}}$, $\mu_{\overline{E[W]}}$.

IV.   PERFORMANCE OF MEASURE

The mean number of customers in the orbit

Based on Zadeh's extension principle $\mu_{\overline{E[O]}}(I)$ is the supremum of minimum over $\{\mu_{\bar{\lambda}}(b), \mu_{\bar{\mu_1}}(c_1), \mu_{\bar{\mu_2}}(c_2), \mu_{\bar{\xi_1}}(d_1), \mu_{\bar{\xi_2}}(d_1) / I = f(b, c_1, c_2, d_1, d_2)\}$

$$I = \frac{b^2 p d_2}{2[bpd_1 + 1]} + \frac{b^2 c_2 + b^2 q d_2 + 2b^2 q d_1 c_1}{2[1 - bc_1 - bqd_1]}$$

to satisfying $\mu_{\overline{E[O]}}(I) = \alpha, \ 0 \le \alpha \le 1$.

We consider the following five cases:
Case(i):$\mu_{\bar{\lambda}}(b) = \alpha, \mu_{\bar{\mu_1}}(c_1) \ge \alpha, \mu_{\bar{\mu_2}}(c_2) \ge \alpha, \mu_{\bar{\xi_1}}(d_1) \ge \alpha, \mu_{\bar{\xi_2}}(d_2) \ge \alpha,$
Case(ii):$\mu_{\bar{\lambda}}(b) \ge \alpha, \mu_{\bar{\mu_1}}(c_1) = \alpha, \mu_{\bar{\mu_2}}(c_2) \ge \alpha, \mu_{\bar{\xi_1}}(d_1) \ge \alpha, \mu_{\bar{\xi_2}}(d_2) \ge \alpha,$
Case(iii):$\mu_{\bar{\lambda}}(b) \ge \alpha, \mu_{\bar{\mu_1}}(c_1) \ge \alpha, \mu_{\bar{\mu_2}}(c_2) = \alpha, \mu_{\bar{\xi_1}}(d_1) \ge \alpha, \mu_{\bar{\xi_2}}(d_2) \ge \alpha,$
Case(iv):$\mu_{\bar{\lambda}}(b) \ge \alpha, \mu_{\bar{\mu_1}}(c_1) \ge \alpha, \mu_{\bar{\mu_2}}(c_2) \ge \alpha, \mu_{\bar{\xi_1}}(d_1) = \alpha, \mu_{\bar{\xi_2}}(d_2) \ge \alpha,$
Case(v):$\mu_{\bar{\lambda}}(b) \ge \alpha, \mu_{\bar{\mu_1}}(c_1) \ge \alpha, \mu_{\bar{\mu_2}}(c_2) \ge \alpha, \mu_{\bar{\xi_1}}(d_1) \ge \alpha, \mu_{\bar{\xi_2}}(d_2) = \alpha.$

For case (i) the lower and upper bound of α- cuts of $\mu_{\overline{E[O]}}$ can be obtained through the corresponding parametric non-linear programs,

$$[E[O]]_\alpha^{L_1} = \min_\Omega \{[I]\} \text{ and } [E[O]]_\alpha^{U_1} = \max_\Omega \{[I]\}.$$

Similarly, we can calculate the lower and upper bounds of the α-cuts of $\mu_{\overline{E[O]}}$ for the all cases (ii),(iii),(iv) and (v). By considering all the cases simultaneously the lower and upper bounds of the α-cuts of $\overline{[E[O]]}$ can be written as

$$[E[O]]_\alpha^{L} = \min_\Omega \{[I]\} \text{ and } [E[O]]_\alpha^{U} = \max_\Omega \{[I]\}$$

where,

$$\text{I} = \frac{b^2 p d_2}{2[bpd_1 + 1]} + \frac{b^2 c_2 + b^2 q d_2 + 2b^2 q d_1 c_1}{2[1 - bc_1 - bqd_1]}$$

such that

$$[b]_\alpha^L \leq \text{b} \leq [b]_\alpha^U, \quad [c_1]_\alpha^L \leq c_1 \leq [c_1]_\alpha^U, \quad [c_2]_\alpha^L \leq c_2 \leq [c_2]_\alpha^U,$$
$$[d_1]_\alpha^L \leq d_1 \leq [d_1]_\alpha^U \text{ and } [d_2]_\alpha^L \leq d_2 \leq [d_2]_\alpha^U.$$

If both $[E[O]]_\alpha^L$ and $[E[O]]_\alpha^U$ are invertible with respect to α, the left and right shape function, $L(I) = [E[O]_\alpha^L]^{-1}$ and $R(I) = [E[O]_\alpha^U]^{-1}$ can be derived from which the membership function $\mu_{\overline{E[O]}}(I)$ can be constructed as

$$\mu_{\overline{E[O]}}(I) = \begin{cases} L(I), & [E[O]]_{\alpha=0}^L \leq I \leq [E[O]]_{\alpha=1}^L \\ 1, & [E[O]]_{\alpha=1}^L \leq I \leq [E[O]]_{\alpha=1}^U \\ R(I), & [E[O]]_{\alpha=1}^U \leq I \leq [E[O]]_{\alpha=0}^U \end{cases} \quad (5)$$

The mean number of customers in the system

We can calculate the lower and upper bounds of the α-cuts of $[E[S]]$ as, $\mu_{\overline{E[S]}}(J)$ is the supremum of minimum over

$$\{\mu_{\bar{\lambda}}(b), \mu_{\bar{\mu}_1}(c_1), \mu_{\bar{\mu}_2}(c_2), \mu_{\bar{\xi}_1}(d_1), \mu_{\bar{\xi}_2}(d_1)/J = f(b, c_1, c_2, d_1, d_2)\}$$

$$[E[S]]_\alpha^L = \min_\Omega \{[J]\} \text{ and } [E[S]]_\alpha^U = \max_\Omega \{[J]\}$$

where,

$$\text{J} = bc_1 + \frac{2b^2 c_1 d_1 + b^2 d_2 + b^2 c_2}{2[1 - b(c_1 + d_1)]}$$

such that
$$[b]^L_\alpha \leq \text{b} \leq [b]^U_\alpha, \quad [c_1]^L_\alpha \leq c_1 \leq [c_1]^U_\alpha, \quad [c_2]^L_\alpha \leq c_2 \leq [c_2]^U_\alpha,$$
$$[d_1]^L_\alpha \leq d_1 \leq [d_1]^U_\alpha \text{ and } [d_2]^L_\alpha \leq d_2 \leq [d_2]^U_\alpha.$$

If both $[E[S]]^L_\alpha$ and $[E[S]]^U_\alpha$ are invertible with respect to α, the left and right shape function, $L(J) = [E[S]^L_\alpha]^{-1}$ and $R(J) = [E[S]^U_\alpha]^{-1}$ can be derived from which the membership function $\mu_{\overline{E[S]}}(J)$ can be constructed as,

$$\mu_{\overline{E[S]}}(J) = \begin{cases} L(J), & [E[S]]^L_{\alpha=0} \leq J \leq [E[S]]^L_{\alpha=1} \\ 1, & [E[S]]^L_{\alpha=1} \leq J \leq [E[S]]^U_{\alpha=1} \\ R(J), & [E[S]]^U_{\alpha=1} \leq J \leq [E[S]]^U_{\alpha=0} \end{cases} \tag{6}$$

The mean number of customers in the waiting time

We can calculate the lower and upper bounds of the α-cuts of $[E[W]]$ as, $\mu_{\overline{E[W]}}(K)$ is the supremum of minimum over
$$\{\mu_{\bar{\lambda}}(b), \mu_{\bar{\mu}_1}(c_1), \mu_{\bar{\mu}_2}(c_2), \mu_{\bar{\xi}_1}(d_1), \mu_{\bar{\xi}_2}(d_1) / K = f(b, c_1, c_2, d_1, d_2)\}$$

$$[E[W]]^L_\alpha = \min_{\Omega}\{[K]\} \text{ and } [E[W]]^U_\alpha = \max_{\Omega}\{[K]\}$$
where,

$$\text{K} = c_1 + \frac{2bc_1d_1 + bd_2 + bc_2}{2[1 - b(c_1 + d_1)]}$$

such that
$$[b]^L_\alpha \leq \text{b} \leq [b]^U_\alpha, \quad [c_1]^L_\alpha \leq c_1 \leq [c_1]^U_\alpha, \quad [c_2]^L_\alpha \leq c_2 \leq [c_2]^U_\alpha,$$
$$[d_1]^L_\alpha \leq d_1 \leq [d_1]^U_\alpha \text{ and } [d_2]^L_\alpha \leq d_2 \leq [d_2]^U_\alpha.$$

If both $[E[W]]^L_\alpha$ and $[E[W]]^U_\alpha$ are invertible with respect to α, the left and right shape function, $L(K) = [E[W]]^L_\alpha]^{-1}$ and $R(K) = [E[W]]^U_\alpha]^{-1}$ can be derived from which the membership function $\mu_{\overline{E[W]}}(K)$ can be constructed as,

$$\mu_{\overline{E[W]}}(K) = \begin{cases} L(K), & [E[W]]^L_{\alpha=0} \leq K \leq [E[W]]^L_{\alpha=1} \\ 1, & [E[W]]^L_{\alpha=1} \leq K \leq [E[W]]^U_{\alpha=1} \\ R(K), & [E[W]]^U_{\alpha=1} \leq K \leq [E[W]]^U_{\alpha=0} \end{cases} \tag{7}$$

V.   NUMERICAL STUDY

The mean number of customers in the orbit

Suppose the fuzzy arrival rate λ, service rate μ_1, μ_2, vacation rate $\overline{\xi_1}$, $\overline{\xi_2}$ are assumed to be hexagonal fuzzy numbers described by

$\overline{\lambda} = [11, 12, 13, 14, 15, 16]$, $\overline{\mu_1} = [13, 14, 15, 16, 17, 18]$, $\overline{\mu_2} = [41, 42, 43, 44, 45, 46]$,
$\overline{\xi_1} = [91, 92, 93, 94, 95, 96]$ and $\overline{\xi_2} = [101, 102, 103, 104, 105, 106]$ per hour respectively.
Then,

$$\lambda(\alpha) = \{ \min_{x \in s(\bar{\lambda})} \{x \in s(\bar{\lambda}), G(x) \geq \alpha\}, \max_{x \in s(\bar{\lambda})} \{x \in s(\bar{\lambda}), G(x) \geq \alpha\}\},$$

where,

$$
G(x) = \begin{cases}
\dfrac{1}{2}\left(\dfrac{x - a_1}{a_2 - a_1}\right), & \text{for} & a_1 \leq x \leq a_2 \\
\dfrac{1}{2} + \dfrac{1}{2}\left(\dfrac{x - a_1}{a_3 - a_2}\right), & \text{for} & a_2 \leq x \leq a_3 \\
1, & \text{for} & a_3 \leq x \leq a_4 \\
1 - \dfrac{1}{2}\left(\dfrac{x - a_4}{a_3 - a_4}\right), & \text{for} & a_4 \leq x \leq a_5 \\
\dfrac{1}{2}\left(\dfrac{a_6 - x}{a_6 - a_5}\right), & \text{for} & a_5 \leq x \leq a_6 \\
0, & \text{for} & \text{otherwise}
\end{cases}
\tag{8}
$$

That is, $\lambda(\alpha) = [11 + \alpha, 16 - \alpha]$, $\mu_1(\alpha) = [13 + \alpha, 18 - \alpha]$, $\mu_2(\alpha) = [41 + \alpha, 46 - \alpha]$, $\xi_1(\alpha) = [91 + \alpha, 96 - \alpha]$ and $\xi_2(\alpha) = [101 + \alpha, 106 - \alpha]$.

It is clear that, when $b = b_\alpha^U$, $c_1 = c_{1\alpha}^U$, $c_2 = c_{2\alpha}^U$, $d_1 = d_{1\alpha}^U$ and $d_2 = d_{2\alpha}^U$, I attains its maximum value and when $b = b_\alpha^L$, $c_1 = c_{1\alpha}^L$, $c_2 = c_{2\alpha}^L$, $d_1 = d_{1\alpha}^L$ and $d_2 = d_{2\alpha}^L$, I attains its minimum value.

From the generated for the given input values of $\overline{\lambda}$, $\overline{\mu_1}$, $\overline{\mu_2}$, $\overline{\xi_1}$, $\overline{\xi_2}$,

(i) For fixed values of b,c_1,c_2 and d_1 I decreases as d_2 increase.
(ii) For fixed values of c_1,c_2,d_1 and d_2 I decreases as b increase.
(iii) For fixed values of b,c_2,d_1 and d_2 I decreases as c_1 increase.
(iv) For fixed values of b,c_1,d_1 and d_2 I decreases as c_2 increase.
(v) For fixed value of b,c_1,c_2 and d_2 I decreases as d_1 increase.

The minimum value of occurs when x-takes its lower bound.
i.e)., $b = 11 + \alpha$ and c_1, c_2, d_1 and d_2 takes their upper bounds given by $c_1 = 18 - \alpha$, $c_2 = 46 - \alpha$, $d_1 = 96 - \alpha$, and $d_2 = 106 - \alpha$ respectively, and the maximum value of E[O] occurs when $b = 16 - \alpha$, $c_1 = 13 + \alpha$, $c_2 = 41 + \alpha$, $d_1 = 91 + \alpha$ and $d_2 = 101 + \alpha$. If both $[E[O]]_\alpha^L$ and $[E[O]]_\alpha^U$ are invertible with respect to 'α' then, the left shape function $L(I) = [E[O]_\alpha^L]^{-1}$ and right shape function $R(I) = [E[O]_\alpha^U]^{-1}$ can be obtained and from

---

which the membership function $\mu_{\overline{E[O]}}(I)$ can be constructed as

$$\mu_{\overline{E[O]}}(I) = \begin{cases} 0.5(x-1), & \text{for} & I_1 \leq I \leq I_2 \\ 0.5 + 0.5(x-1), & \text{for} & I_2 \leq I \leq I_3 \\ 1, & \text{for} & I_3 \leq I \leq I_4 \\ 1 + 0.5(x-4), & \text{for} & I_4 \leq I \leq I_5 \\ 0.5(6-x) & \text{for} & I_5 \leq I \leq I_6 \\ 0, & \text{for} & \text{otherwise} \end{cases} \qquad (9)$$

For the given set of input values, the values of I_1, I_2, I_3, I_4, I_5 and I_6 evaluated c programme given above are 0.000, 8.717, 9.264, 9.154, 8.826 and 0.000 respectively and

$$\mu_{\overline{E[O]}}(I) = \begin{cases} 0.5(x-1), & \text{for} & 0.000 \leq I \leq 8.717 \\ 0.5 + 0.5(x-1), & \text{for} & 8.717 \leq I \leq 9.264 \\ 1, & \text{for} & 9.264 \leq I \leq 9.154 \\ 1 + 0.5(x-4), & \text{for} & 9.154 \leq I \leq 8.826 \\ 0.5(6-x) & \text{for} & 8.826 \leq I \leq 0.000 \\ 0 & \text{for} & \text{otherwise} \end{cases} \qquad (10)$$

The graphs of the shape function L(I) and R(I) are given in the figure 1

The mean number of customers in the system

The minimum value of occurs when x-takes its lower bound.
i.e)., $b = 11 + \alpha$ and c_1, c_2, d_1 and d_2 takes their upper bounds given by $c_1 = 18 - \alpha$, $c_2 = 46 - \alpha$, $d_1 = 96 - \alpha$ and $d_2 = 106 - \alpha$ respectively and the maximum value of E[S] occurs when $b = 16 - \alpha$, $c_1 = 13 + \alpha$, $c_2 = 41 + \alpha$, $d_1 = 91 + \alpha$ and $d_2 = 101 + \alpha$. If both $[E[S]]_\alpha^L$ and $[E[S]]_\alpha^U$ are invertible with respect to 'α' then, the left shape function $L(J) = [E[S]_\alpha^L]^{-1}$ and right shape function $R(J) = [E[S]_\alpha^U]^{-1}$ can be obtained and from which the membership function $\mu_{\overline{E[S]}}(J)$ can be constructed as:

$$\mu_{\overline{E[S]}}(J) = \begin{cases} 0.5(x-1), & \text{for} & J_1 \le J \le J_2 \\ 0.5 + 0.5(x-1), & \text{for} & J_2 \le J \le J_3 \\ 1, & \text{for} & J_3 \le J \le J_4 \\ 1 + 0.5(x-4), & \text{for} & J_4 \le J \le J_5 \\ 0.5(6-x) & \text{for} & J_5 \le J \le J_6 \\ 0, & \text{for} & \text{otherwise} \end{cases} \tag{11}$$

For the given set of input values, the values of J_1, J_2, J_3, J_4, J_5 and J_6 evaluated c programme given above are 0.8462, 1.9776, 2.0829, 2.0847, 1.9793 and 0.8710 respectively and

$$\mu_{\overline{E[S]}}(J) = \begin{cases} 0.5(x-1), & \text{for} & 0.8462 \le J \le 1.9776 \\ 0.5 + 0.5(x-1), & \text{for} & 1.9776 \le J \le 2.0829 \\ 1, & \text{for} & 2.0829 \le J \le 2.0847 \\ 1 + 0.5(x-4), & \text{for} & 2.0847 \le J \le 1.9793 \\ 0.5(6-x) & \text{for} & 1.9793 \le J \le 0.8710 \\ 0 & \text{for} & \text{otherwise} \end{cases} \tag{12}$$

The graphs of the shape function L(J) and R(J) are given in the figure 2

The mean number of customers in the waiting time

The minimum value of occurs when x-takes its lower bound.
i.e)., $b = 11 + \alpha$ and c_1, c_2, d_1 and d_2 takes their upper bounds given by $c_1 = 18 - \alpha$, $c_2 = 46 - \alpha$, $d_1 = 96 - \alpha$ and $d_2 = 106 - \alpha$ respectively and the maximum value of E[W] occurs when $b = 16 - \alpha$, $c_1 = 13 + \alpha$, $c_2 = 41 + \alpha$, $d_1 = 91 + \alpha$ and $d_2 = 101 + \alpha$. If both $[E[W]]_\alpha^L$ and $[E[W]]_\alpha^U$ are invertible with respect to 'α' then, the left shape function $L(K) = [E[W]_\alpha^L]^{-1}$ and right shape function $R(K) = [E[W]_\alpha^U]^{-1}$ can be obtained and from which the membership function $\mu_{\overline{E[W]}}(K)$ can be constructed as:

$$\mu_{\overline{E[W]}}(K) = \begin{cases} 0.5(x-1), & \text{for} & K_1 \leq K \leq K_2 \\ 0.5 + 0.5(x-1), & \text{for} & K_2 \leq K \leq K_3 \\ 1, & \text{for} & K_3 \leq K \leq K_4 \\ 1 + 0.5(x-4), & \text{for} & K_4 \leq K \leq K_5 \\ 0.5(6-x) & \text{for} & K_5 \leq K \leq K_6 \\ 0, & \text{for} & \text{otherwise} \end{cases} \qquad (13)$$

For the given set of input values, the values of K_1, K_2, K_3, K_4, K_5 and K_6 evaluated c programme given above are 0.0000, 13.5398, 14.1564, 14.4615, 13.8491 and 0.0000 respectively and

$$\mu_{\overline{E[W]}}(K) = \begin{cases} 0.5(x-1), & \text{for} & 0.0000 \leq K \leq 13.5398 \\ 0.5 + 0.5(x-1), & \text{for} & 13.5398 \leq K \leq 14.1564 \\ 1, & \text{for} & 14.1564 \leq K \leq 14.4615 \\ 1 + 0.5(x-4), & \text{for} & 14.4615 \leq K \leq 13.8491 \\ 0.5(6-x) & \text{for} & 13.8491 \leq K \leq 0.0000 \\ 0 & \text{for} & \text{otherwise} \end{cases} \qquad (14)$$

The graphs of the shape function L(K) and R(K) are given in the figure 3

In this paper we fix the service rate $\bar{\mu}_2$ by crisp value 43.5 and taking arrival rate $\overline{\lambda} = [11, 12, 13, 14, 15, 16]$, service rate $\overline{\mu_1} = [13, 14, 15, 16, 17, 18]$ both hexagonal fuzzy numbers and the values of the mean number of customer in the orbit were generated and from the figure 6.1. It is observed that as $\overline{\lambda}$ increases the mean number of customer in the orbit increases for the fixed value of the service rate. Whereas for fixed value of arrival rate, the mean number of customer in the orbit decreases as service rate increases. It is also observed from the data generated that, the membership value of the mean number of customer in the orbit is 9.4, when the ranges of arrival rate, service rate lie in the intervals $(13, 14.4)$, $(15.5, 16.5)$ respectively.

For fixed value of $\xi_1 = 93$ and 93.3 the graph of the mean number of customer in the system drawn in figure 6.2 shows that, as arrival rate increases the mean number of customer in the system also increases, while the vacation time decreases as the mean number of customer in the system increases. It is also observed from the data generated that, the membership value of the mean number of customer in the system is 2.1, when the ranges of arrival rate, service rate, and the working vacation rate lie in the intervals $(13.5, 14.3)$, $(93, 94.3)$ respectively.

Again for fixed values of $\xi_2 = 102.5$ and 103.7 the graph of the mean reneging rate of the system are drawn in figure 6.3 respectively. This figure shows that as arrival rate increases, also the mean number of customer in the waiting time increases, while the the mean number of customer in the waiting time decreases as the service rate increases. It is also observed from the data generated, that the membership value of the the mean number of customer in the waiting time is 15.06, when the ranges of arrival rate, service rate, and the vacation rate lie the intervals $(12.5, 13.8)$, $(102, 104.6)$ respectively.

The following three graphs are represent the performance mea- sures
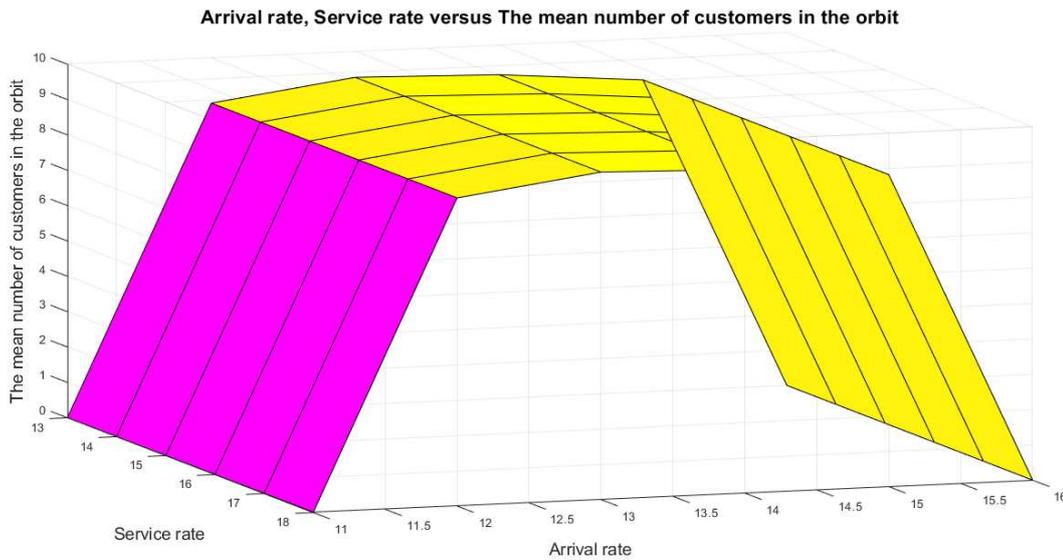
Figure 1: Arrival Rate, Service Rate Versus the Mean Number of Customer in the Orbit
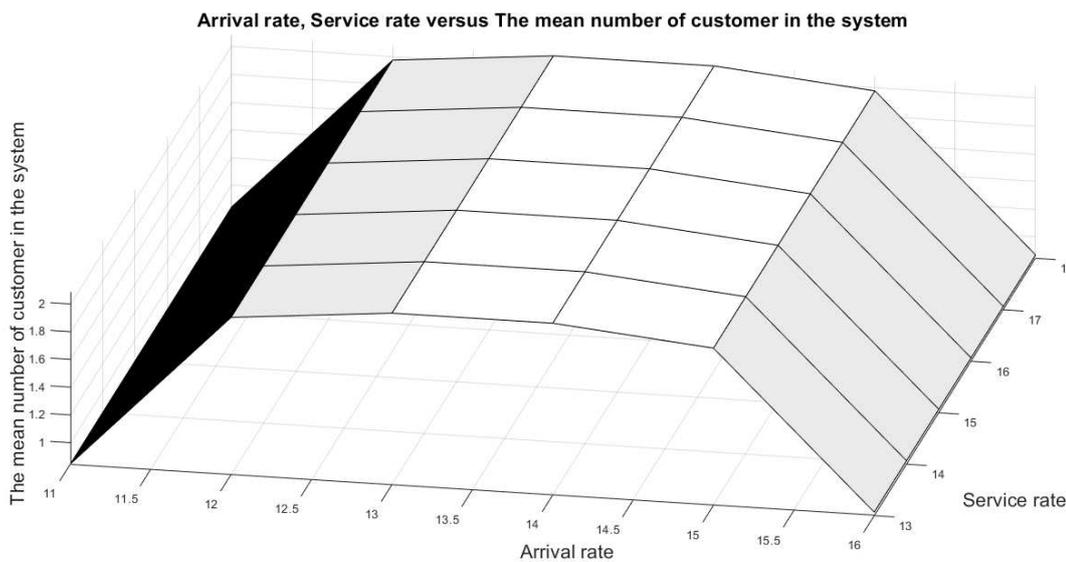
Figure 2: Arrival Rate, Service Rate Versus the Mean Number of Customer in the System
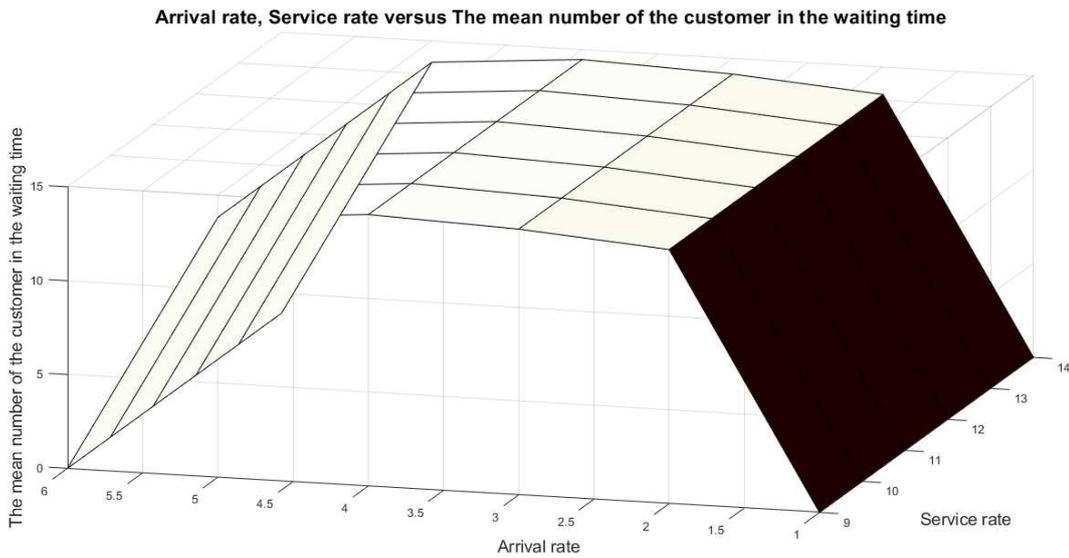
Analysis of FM/FG/1 Retrial Queue with Bernoulli Schedule and Vacation using Hexagonal Fuzzy Numbers

Arrival rate, Service rate versus The mean number of the customer in the waiting time

Figure 3: Arrival Rate, Service Rate Versus the Mean Number of Customer in the Waiting Time

VI. CONCLUSION

In this paper we have studied analysis of FM/FG/1 retrial queue with Bernoulli schedule and vacation using hexagonal fuzzy numbers. Based on Zadeh's extension principle, system performances of interest for the mean number of customers in the orbit, the mean number of customers in the system and the mean number in the waiting time. We have obtained numerical results to all the performances and graphs to the corresponding measures are obtained. Basically, queue formation is a phenomenon that often occurs when the current demand for a service excees the current capacity to offer that service. This fuzzy retrial queueing systems are useful everywhere in the society. The capablity of these systems can have an impact result on the quality of human lives and productivity of the process. Fuzzy retrial queueing systems were applied to procure the performance analysis of different system like telephone switching systems, computers competing to gain service from a central processing unit etc., Fuzzy retrial queues are more realistic when compared to crisp queues.

REFERENCES

1. T.Y ang and H.Li, The M/G/1 retrial queue with the server subject to starting failures, queuing systems, 16, 83-96, 1994.
2. R.J Lie and E.S Lee (1989), Analysis of fuzzy queues computers an mathematics with applications.
3. J.C. Ke, H.I Huang and C.H.Lin, On retrial queuing model with fuzzy parameter, physic A 374 (2007), 272-280.
4. D.S Negi and E.S Lee,(1992), Analysis and simulation of fuzzy queue fuzzy sets and Systems 46 321-330.
5. K.Dhurai, A.Karpagam, A new membership function on hexagonal fuzzy numbers. Vol- ume 5 Issue 5,(2016).
6. L.A Zadeh,(1978) Fuzzy sets as a basis a theory of possibility, fuzzy sets and systems. 1.pp.3-28.
7. W.Rita and L.Robert, Application of fuzzy set theory to retrial queues. International journal of algorithms computing and mathematics 2(4)(2009), 9-18.

This page is intentionally left blank

Dependence of Fuel Economy on Speed for two Heavy Duty Vehicles

N. Dominguez-Vergara, D.N. Dominguez-Perez & J.L. Pantoja-Gallegos

Universidad Autónoma Metropolitana

Universidad Nacional Autónoma de México

ABSTRACT

Some recommendations have been made that vehicles should travel at certain speeds in order to reduce their fuel consumption because gasoline and diesel are currently very expensive in many countries. There is also the menace of fuel shortages approaching the near future in some parts of the world. These recommendations are based on the fact that on the road the fuel economy of a vehicle increases while travelling at cruise speed without acceleration, as it is shown in this paper. Some of the vehicles on the road are the heavy-duty vehicles which transport people, food, medicine, minerals, gasoline, diesel, and many other goods to keep the economy of any country running. The vast majority of heavy-duty vehicles on the road in the world still move with diesel engines. In this paper it is demonstrated, for the cases examined with heavy duty vehicles, that the fuel economy of vehicles depends on several factors which include the load transported, the acceleration to reach cruise speed, the engine, the gearbox, the wheels, the final drive, the maximum driving speed of the vehicles and the slope of the roads. The reduction of fossil fuels consumption in road transportation also reduces the emision of carbon dioxide to the atmosphere, a greenhouse gas which contributes to global climate change. For some of the cases studied the carbon dioxide emissions are also calculated. Savings in fuel consumption in dollars by driving at the best constant speeds and the reduction in the environmental cost caused by less emissions of carbon dioxide are reported.

Keywords: fuel economy, heavy duty vehicles, driving cycle, global climate change.

Classification: DDC Code: 333.794 LCC Code: TP359.H8

Language: English

Dependence of Fuel Economy on Speed for two Heavy Duty Vehicles

N. Dominguez-Vergara [1*], D.N. Dominguez-Perez[2] & J.L. Pantoja-Gallegos[1]

ABSTRACT

Some recommendations have been made that vehicles should travel at certain speeds in order to reduce their fuel consumption because gasoline and diesel are currently very expensive in many countries. There is also the menace of fuel shortages approaching the near future in some parts of the world. These recommendations are based on the fact that on the road the fuel economy of a vehicle increases while travelling at cruise speed without acceleration, as it is shown in this paper. Some of the vehicles on the road are the heavy-duty vehicles which transport people, food, medicine, minerals, gasoline, diesel, and many other goods to keep the economy of any country running. The vast majority of heavy-duty vehicles on the road in the world still move with diesel engines. In this paper it is demonstrated, for the cases examined with heavy duty vehicles, that the fuel economy of vehicles depends on several factors which include the load transported, the acceleration to reach cruise speed, the engine, the gearbox, the wheels, the final drive, the maximum driving speed of the vehicles and the slope of the roads. The reduction of fossil fuels consumption in road transportation also reduces the emision of carbon dioxide to the atmosphere, a greenhouse gas which contributes to global climate change. For some of the cases studied the carbon dioxide emissions are also calculated. Savings in fuel consumption in dollars by driving at the best constant speeds and the reduction in the environmental cost caused by less emissions of carbon dioxide are reported. The calculations in this paper have been carried out using UAMmero, a computer program developed at the Mexican Universidad Autónoma Metropolitana. The results are presented for two heavy duty vehicles with 455 HP and 200 HP engines respectively, moving in two parts of a driving cycle used by the United States of America Environmental Protection Agency and the National Highway Transportation and Safety Agency to certify compliance of heavy duty vehicles to the fuel consumption and carbon dioxide emissions regulations in that country, as well as for the case in which they move with constant speed.

I. INTRODUCTION

The current rapid increase in the demand for oil and its world production inferior to the COVID-19 pre-pandemic level has led to oil prices above $100 United States of America (US) dollars per barrel in the world during several weeks in the first quarter of the year of 2022. Consequently, the prices for gasoline and diesel in the US and in some countries of Europe have reached maximum prices above $5 US dollars per gallon. Nowadays, some countries consider reducing its dependence on Russian oil which is also impacting the price of oil-bearing products and could even lead to shortages of fuels for transportation in some European countries and others. On top of that, the possibility of attacks against petroleum installations, natural disasters in oil exporting countries and wars around the world cause uncertainty in the prices of petroleum. Therefore, there is the need of reducing the fuel consumption of the vehicles on the road; among these are the heavy-duty vehicles which transport people and goods necessary for most of the economic activities of all the countries. The heavy-duty vehicles are so important that when there are not enough heavy-duty drivers on the road or when

they do not work, for any reason, there are shortages in food, fuels and other goods as how a few countries have experienced recently. Most of the heavy-duty vehicles on the road in the world move with diesel engines; cleaner fuels or electric or hybrid heavy duty vehicles are not yet available or affordable. Furthermore, some countries rely on fleets of old vehicles, like in Mexico where heavy-duty vehicles have an average age of 17 years. Recently, there have been recommendations stating that to save fuels and money in road trips, automotive vehicles should be driven at specific speeds. However, in this paper it is demonstrated, for the cases studied with heavy duty vehicles, that the fuel economy depends on several factors which include the load transported, the acceleration to reach the cruise speed, the cruise speed, the engine fuel consumption with respect to the revolutions per minute of the engine (rpm) and the slope of the roads. Since decades ago, many countries have had the goal of reducing their fossil fuel consumption in the transportation sector to increase their energy security because they do not produce enough oil (like most of the European countries and the US) or refined petroleum products because they do not have enough refineries (like Mexico since the year of 1990). Another very important reason to reduce fossil fuel consumption in road transportation is the concern of global climate change because the combustion of fossil fuels produces carbon dioxide (CO_2) emissions which is a greenhouse gas. Due to these and other concerns like the deterioration of the air quality, there are currently several efforts to regulate the fuel economy and the CO_2 emissions of new light and heavy-duty vehicles around the world, although not many countries have imposed good mandatory regulations on them. For example, in the US, a new regulation will mandate that the new fleet of automobiles and light trucks reach a Corporate Average Fuel Economy of 49 miles/gallon or 20.83 kilometers (km) per liter by the year 2026. In the European Union, Japan, Canada, and the US, among a few other places, federal regulations on those matters have been implemented for new heavy-duty vehicles. The Greenhouse Gas

Emissions Model (GEM) [1], a computer program, was created to test compliance of heavy-duty vehicles to the US regulations and VECTO [2], another computer program, is being developed to test those vehicles to the regulations in the European Union. In Mexico, UAMmero is being developed [3] with different programming schemes from those of GEM and VECTO to evaluate fuel consumption and CO_2 emissions of heavy-duty vehicles; although there is not yet a Mexican federal regulation on those two variables but only some governmental programs to increase the fuel economy of heavy-duty vehicles [4]. UAMmero is being developed using free software and it does not require proprietary software to run it. UAMmero has been developed in C language and shows many of its results graphically. Some results from UAMmero have been compared with those out of GEM [3]. Most of the results of UAMmero have been obtained for a driving cycle that the US Environmental Protection Agency (EPA) and the National Highway Transport and Safety Administration (NHTSA) use to certify heavy duty vehicles to fuel consumption and CO_2 emissions [1]. UAMmero also calculates the fuel consumption and CO_2 emissions of heavy-duty vehicles travelling in highways, although until now only a very few of these results have been published. In this work the fuel economy and CO_2 emissions are calculated for two different heavy-duty vehicles moving in two parts of a driving cycle starting from speed zero and reaching their cruise speed. One of the two vehicles has a 455 Horse Power (HP) engine and the other a 200 HP engine, the first of the vehicles corresponds to a Class 8 heavy duty vehicle and the second one to a Class 2b-5 heavy duty vehicle. Some other calculations in which the two vehicles move with constant speeds are also reported. The cost of the fuel and that of the environmental damage due to the CO_2 emissions are calculated in order to show the reductions in both by driving at certain speeds. In section 2 the vehicle dynamics and the driving cycle is presented, in section 3 the characteristics of the two heavy duty vehicles are explained, in section 4 the fuel economy and the

CO_2 emissions are reported and finally section 5 contains the conclusions.

II. VEHICLE DYNAMICS AND DRIVING CYCLE

2.1 Forces and torques

The vehicle dynamics is described by Equation 1 [3].

$$(M + m_i)a = \frac{T_e R_{eff}}{r_w} - F_a - F_p - F_r \quad \# \tag{1}$$

The vehicle moves in one direction. In Equation 1, F_a, is the aerodynamic force, F_p is the force due to the slope of the road, F_r is the force due to the friction of the wheels with the pavement of the road. M is the total mass of the vehicle including the load, m_i is the inertial mass of the vehicle. M and m_i are proportionated in kilograms (kg). a is the magnitud of the linear acceleration, r_w is the radius of one wheel (all the wheels have the same radius). T_e is the engine torque necesary to move the vehicle. R_{eff} is the effective ratio of the gear ratio of the gearbox being used by the vehicle in motion combined with the final drive ratio of the vehicle. In this work a heavy-duty vehicle with a 455 HP engine and 10 gear gearbox and a heavy truck with a 200 HP engine and 6 gear gearbox are analized. All the parameters of these two vehicles can be found in the user's guide of GEM 2010 [5] and in the software of GEM developed for the first phase of the regulation in the US. F_a, F_p, and F_r, are calculated using Equations 2, 3 and 4.

$$F_a = \frac{1}{2} c_{air} A_L \rho_a V^2 \quad \# \tag{2}$$

r_w =0.489 meters (m) for the 455 HP heavy duty vehicle and 0.378 m for the 200 HP heavy truck. The speed of the vehicle along the road, V, is given in meters per second (m/s), although in some results is reported in km/hr. In Equation 2, $c_{air} = 0.69$, is the aerodynamic coefficient for the 455 HP heavy duty vehicle and $c_{air} = 0.6$ for the

heavy truck. $\rho_a = 1.1845 \frac{kg}{m^3}$, is the air density. $A_L = 10.4\,m^2$, is the frontal area of the 455 HP heavy duty vehicle and $A_L = 9.0\,m^2$, for the 200 HP heavy truck.

$$F_p = Mg sin(\theta) \quad \# \tag{3}$$
$$F_r = C_r Mg \cos\cos(\theta) \quad \# \tag{4}$$

The mass without load for the heavy-duty vehicle is of $14742\,kg$, the mass for the heavy truck without load is of $4407\,kg$. $g = 9.8066\,\frac{m}{s^2}$, is the acceleration of gravity. θ is the angle of inclination of the road. $C_r = 0.007205$ for the 455 HP heavy duty vehicle and $C_r = 0.0035$ for the 200 HP heavy truck. The frequency of rotation of a wheel, ω_w, is obtained from Equation 5.

$$\omega_w = \frac{V}{r_w} \quad \# \tag{5}$$

The frequency of rotation of the engine, ω_e (or rpm), is obtained from Equation 6.

$$rpm = \omega_e = R_{eff} \omega_w \quad \# \tag{6}$$

The relation between the speed of the vehicle and the rpm of the engine (ω_e) is given in Equation 7.

$$V = r_w \omega_w = \frac{r_w}{R_{eff}} \omega_e \quad \# \tag{7}$$

The engine torque, T_e, to move the vehicle is given in equation 8.

$$T_e = \frac{F r_w}{R_{eff}} \quad \# \tag{8}$$

Where F is defined in Equation 9.

$$F = F_r + F_a + F_p + Ma + m_i a \quad \# \tag{9}$$

F, F_r, F_a, F_p, Ma and $m_i a$ are obtained in Newtons (N). T_e, is obtained in Newtons times meters (N-m). m_i, is defined in Equation 10.

$$m_i = \frac{I_{eff}}{r_w^2} \quad \#$$
(10)

In equation 10, I_{eff} is the effective moment of inertia. The inertial mass involves the rotating parts of the vehicle, like the wheels, the final drive, the clutch and the current gearbox gear used in moving the vehicle. As the vehicle moves, it uses different gears of the gearbox to accelerate or deaccelerate [3] and therefore the inertial mass changes. If the vehicle does not accelerate or deaccelerate there is no change of gears during the trip, although different speeds might require different gears. Different gears have different ratios and therefore R_{eff}, changes as the gears change during the motion of the vehicle. The changes of gears are considered instantaneous.

As the vehicle moves, the rpm and T_e change if the vehicle accelerates or deaccelerates, otherwise they remain constant. Once the rpm and T_e are calculated, the fuel consumption of the vehicle in kg/s is obtained using the engine fuel map which is a table of fuel consumptions for pairs of rpm and T_e. The instantaneous fuel consumption in kg per liter is calculated (considering a diesel density of 0.847 kg/liter), as well as the distance travelled. From the distance travelled and the fuel consumption, the fuel economy is obtained in km per liter (km/liter), because it is the distance travelled over the fuel consumed. The cost of the fuel for the trip is obtained by multiplying the price of a liter of diesel in US dollars by the amount of fuel consumed in liters. The amount of CO_2 emitted in kg is obtained by multiplying the number of liters of diesel consumed in the engine by 2.6 kg/liter, which is the amount of CO_2 emitted for a liter of diesel burned. The environmental cost of the CO_2 emitted is obtained by multiplying the amount of tons (thousands of kg) of CO_2 for the environmental cost of one ton of CO_2 emitted to the atmosphere, which in this work is taken as $12 US dollars.

2.2 Vehicle moving in the two highway parts of a driving cycle

The driving cycle which is used in GEM to certify heavy duty vehicles to fuel consumption and CO_2 emissions is a table of values of the speed of the vehicle with respect to time. The driving cycle consists of three parts; the speed for the first, second and third parts versus time is shown in Figure 1. The first part models the speed of the vehicle in an urban region. The second part simulates the speed of the vehicle in a highway with maximum speed of 55 miles/hr or 88.5139 km/hr. And the third part models the speed of the vehicle which moves in a highway with maximum speed of 65 miles/hr or 104.6074 km/hr. In the first part of the driving cycle, which is the urban region, the vehicle accelerates and deaccelerates constantly whereas in the second and third parts the vehicle starts with zero speed, and then advances with a constant acceleration until it reaches the maximum speed and thereafter advances at that speed for several minutes and finally deaccelerates up to zero speed. In this paper the calculation for the fuel economy and CO_2 emissions is carried out for the parts 2 and 3 of the driving cycle to show that the fuel economy also depends on the acceleration to reach a maximum speed. The calculation of the fuel economy is carried out for parts 2 and 3 of the driving cycle for the parts in which the vehicle accelerates and the parts in which the vehicle moves with the maximum speeds. The maximum speeds for the parts 2 and 3 of the driving cycles are target or objective speeds because they are not reached if the vehicle transports a heavy load or travels in a road with a steep slope; in these cases, the necessary torque to move the vehicle is larger than the maximum torque that the engine can provide. Therefore, in cases in which the necessary torque, T_e, to move the vehicle is larger than the maximum that the engine can provide, $T_{e,max}$, the vehicle acceleration is reduced to the one obtained with the maximum torque that the engine can provide; thus, the resulting maximum speed in which the vehicle moves becomes smaller than the target speed.
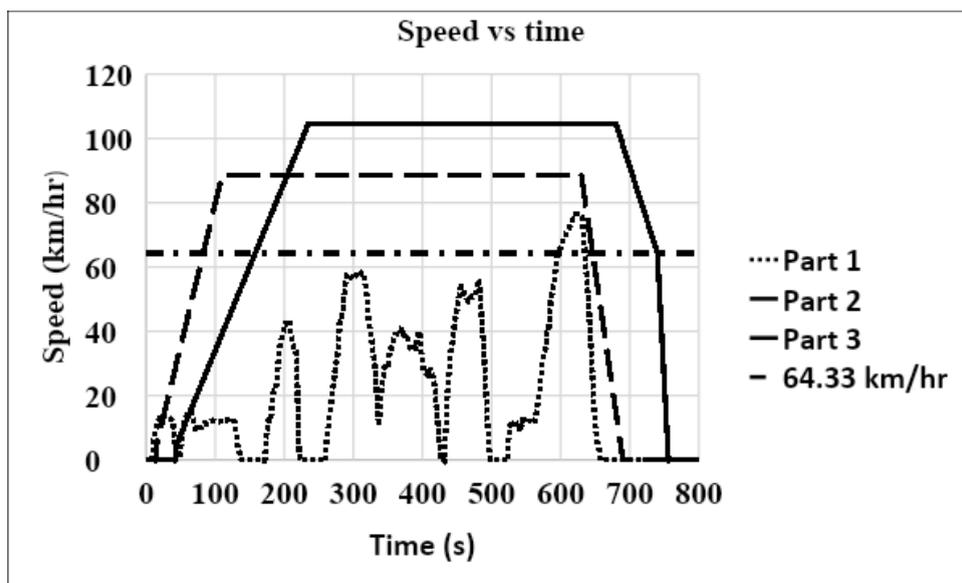
Figure 1: Target speed (km/hr) versus time (s) for parts 1, 2 and 3 of the driving cycle as well as a constant speed of 64.33 km/hr versus time (not part of the driving cycle).

2.3 Vehicle moving with constant speed

Calculations of the fuel economy and CO_2 emissions for the case in which the vehicle moves with constant speed all the time are also presented, see Figure 1 for the constant speed of 64.33 km/hr; although the results are presented for constant speeds from 4 up to 104.6074 km/hr. In these cases, the vehicle does not start moving from zero speed and the vehicle acceleration is zero all the time. In this case the necessary engine torque to move the vehicle is obtained from Equation 11 (because the acceleration is zero).

$$T_e = \frac{\left(F_r + F_a + F_p\right)r_w}{R_{eff}} \#$$ (11)

UAMmero is run for the part 3 of the driving cycle to easily obtain the fuel economy for the constant speed cases. The rpm for any speed of the vehicle is calculated (Equation 7) and then the acceleration is set equal to zero in the calculation of the torque (Equation 11).

After obtaining the rpm and T_e, the fuel consumption is obtained from the array of the fuel map. In the cases of constant speed (no acceleration), the necessary torque to move the vehicle is smaller than in the case when the vehicle accelerates (for same values of the speed); therefore, the fuel consumption is smaller than in the cases in which the vehicle first accelerates to reach the maximum speed. Thus, the fuel economy is larger in the case of constant speed as it is shown in the results below.

III. CHARACTERISTICS OF THE HEAVY-DUTY VEHICLES

In this work the fuel economy and CO_2 emissions are calculated for a 455 HP heavy-duty vehicle and for a 200 HP heavy truck. The mass of the 455 HP heavy duty vehicle without load is of 14742 kg; with a load of 17236 kg, its total mass is of 31978 kg. The mass of the 200 HP without load is of 4407 kg and several loads are considered. The parameters for the engine, gearbox, clutch and wheels for the 455 HP heavy duty vehicle are given elsewhere [3][5]. The parameters for the engine, gearbox and wheels for the 200 HP heavy truck have been also proportionated elsewhere [5]. The fuel consumptions by the engines are provided by fuel maps, which were directly obtained for the two vehicles from the data of the first version of the software of GEM.

3.1 455 HP Heavy Duty Vehicle

The maxima of the maximum torque, $T_{e,max}$, the maximum power, $P_{e,max}$ (equal to 0.745699872* $T_{e,max}$*rpm), as well as for the specific fuel consumption (SC) for $T_{e,max}$ (SC_{max}), as a function

---

of rpm, proportionated by the 455 HP engine are: 2100 N-m (at rpm=1200 and rpm=1250), 455.26066 HP (at rpm=1800) and 0.0000505376 kg/(HP*s) respectively. The engine specific fuel consumption (SC) is obtained by dividing the fuel consumption over the engine power. The normalized values with respect to their maxima of $T_{e,max}$, $P_{e,max}$, and SC_{max}, are shown in Figure 2.
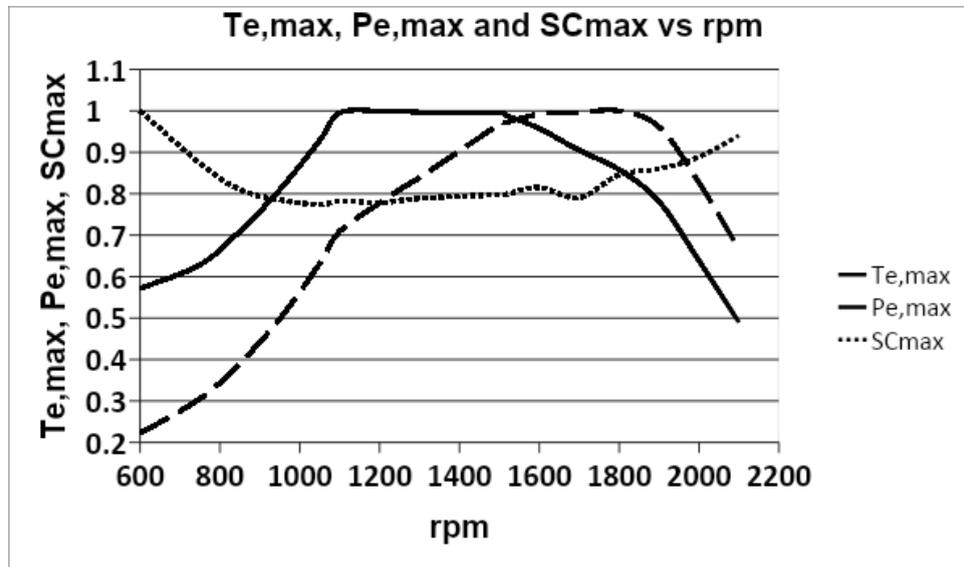

Figure 2: $T_{e,max}$, $P_{e,max}$ and the values of the specific fuel consumption for $T_{e,max}$ versus rpm, for the 455 HP heavy duty vehicle.

The range of values of rpm, are determined by the speed at which the vehicle travels, the values of the speeds at which the vehicle changes gears, the radius of the wheels, and by the values of the effective ratios of the relations of the gears (Equation 7) [3]. During the driving, the rpm used in moving the vehicle are located, most of the time of operation of the heavy duty vehicles, around the values which produce the maximum of the torque and the minimum of the specific fuel consumption; that is how the heavy duty vehicles are designed, to be driven around the maximum of the torque because of the heavy loads that they transport and in the region of the minimim of the specific fuel consumption.

3.2 200 HP heavy truck

The maxima of the maximum torque, $T_{e,max}$, the maximum power, $P_{e,max}$, as well as the specific fuel consumption for $T_{e,max}$, as a function of rpm, proportionated by the 200 HP engine are: 7300 N-m (at rpm=1300, 1500, 1600 and 1800), 200.25964 HP (at rpm=2000) and 0.0000938264 kg/(HP*s) respectively. The normalized values with respect to their maxima of $T_{e,max}$, $P_{e,max}$, and SC_{max}, are shown in Figure 3.
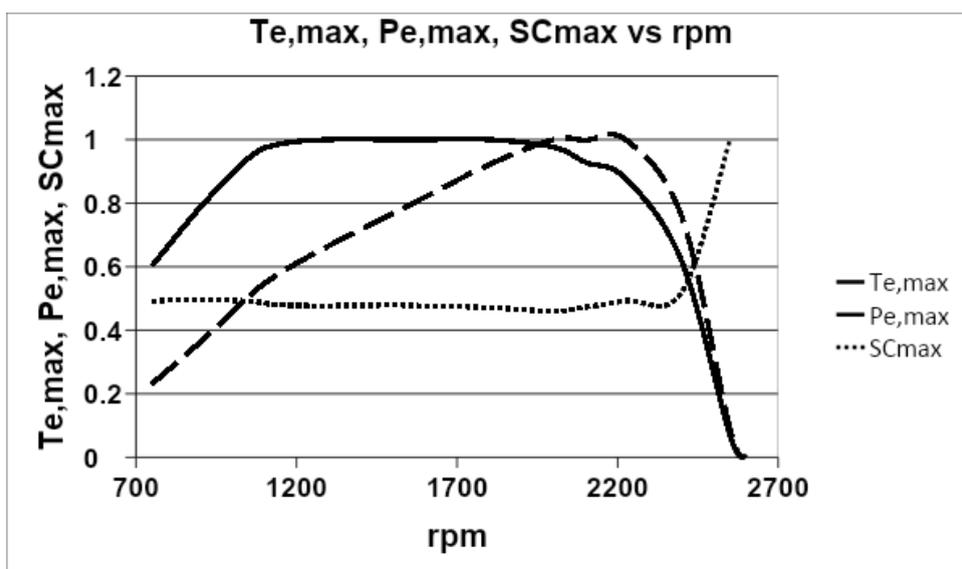
Figure 3: $T_{e,max}$, $P_{e,max}$ and the values of the specific fuel consumption for $T_{e,max}$ versus rpm, for the 200 HP heavy truck.

IV. FUEL ECONOMY

In this section the results for fuel economy for the 455 HP heavy duty vehicle and for the 200 HP heavy truck are presented.

4.1 455 HP heavy duty vehicle moving in a road with zero slope

In this section the results for the fuel economy for the 455 HP heavy duty vehicle moving in parts 2 and 3 of the driving cycle and with constant speeds are compared. The T_e is obtained from Equation 8 which depends on F (Equation 9). In Figure 4 the values of F_a, F_r, Ma and $m_i a$ are shown as a function of the speed for the 455 HP heavy duty vehicle, for 0° of the inclination of the road, M= 31978 kg and the part 3 of the driving cycle; F_p is not shown because is equal to zero.
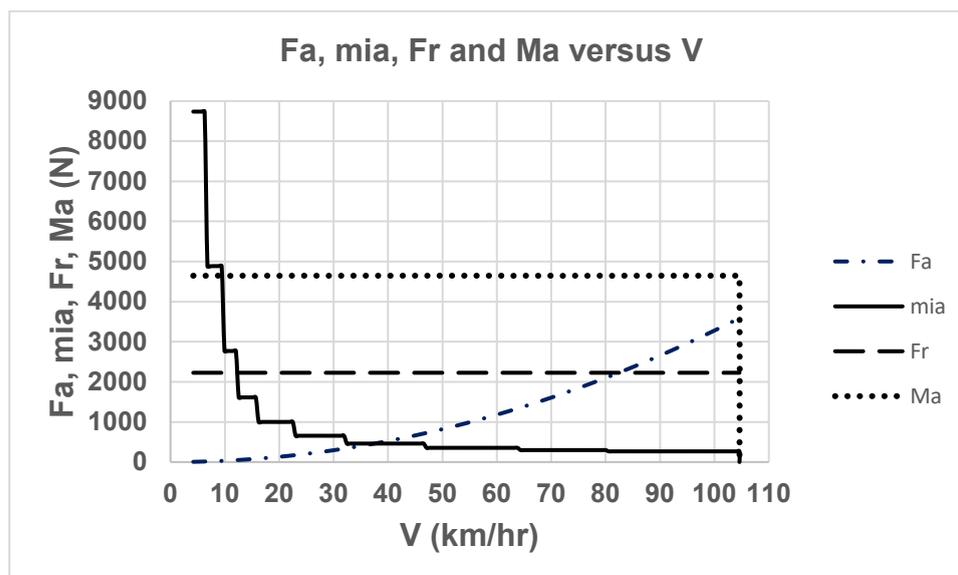

Figure 4: F_a, F_r, Ma and $m_i a$ versus the speed of the vehicle for the case of 0° of inclination of the road, M= 31978 kg and the part 3 of the driving cycle.

F_a, the aerodynamic force increases cuadratically as the speed increases as it is seen in Figure 4. Ma is constant because, a, the acceleration is constant and larger than zero ($a = 0.1453\ \frac{m}{s^2}$) except in the part in which the vehicle travels at constant speed of 104.6074 km/hr; at this constant speed the acceleration is zero and Ma becomes zero. F_r is constant because it does not depend on the speed. The inertial mass, m_i, changes as the vehicle accelerates and changes gears because they have different ratios. In this case, m_i decreases as the vehicle changes gears from the first to the tenth. $m_i a$ is the value of m_i multiplied by the constant value of a until the vehicle starts moving with constant speed, and in this last part $m_i a$ is equal to zero because the acceleration is zero.

For the part 2 of the driving cycle, the maximum speed reached is of 86.6081 km/hr; a little less than the target speed of 88.5139 km/hr. F_r and F_a have the same values as for the part 3 of the driving cycle up to the maximum speed which in this case is of 86.6081 km/hr; Ma and $m_i a$ have the same shape as for the case of the part 3 of the driving cycle but their values are larger in the part in which the acceleration is constant and larger than zero, because in this case $a = 0.2459\ \frac{m}{s^2}$, except very close to the part of constant speed because the needed torque for those values of the speed is larger than $T_{e,\ max}$ and therefore the acceleration has to be reduced which leads to a smaller speed than the target speed of 88.5139 km/hr. F_p is also zero because the road has an inclination of 0°.

For the case in which the vehicle travels at any constant speed during its whole trip, the values of $F_a, F_r,\ F_p, Ma\ and\ m_i a$ would be represented by a single points in Figure 4, because the vehicle travels at just one (constant) speed. And in this case, both Ma and $m_i a$ are equal to zero because the acceleration is zero. F_p is zero because the inclination of the road is zero. F_r and F_a have the

values that they have for part 3 of the driving cycle for the same value of the speed. The results below are obtained not just for one value of a constant speed but for constant speeds from 4 up to 104.6074 km/hr.

In Figure 5 the value of F is shown as a function of the speed for the two parts of the driving cycle and for the case in which the vehicle moves with constant speed (for a range of constant speeds from 4 to 104.6074 km/hr). For the case in which the speeds are constant from 4 to 104.6074 km/hr their values of F are smaller than the value of F for the two parts of the driving cycle in which the vehicle accelerates, as it can be seen in Figure 5, because the two parts of the driving cycle include Ma and $m_i a$, which are zero in the cases of constant speed. Thus, F is smaller (for the same value of the speed) for the case in which the vehicle travels at constant speed. Also, the value of F is smaller for the part 3 of the driving cycle when the vehicle is accelerating, than for the part 2, because the acceleration is smaller for the part 3 as it can be seen in Figure 5. That is, if the vehicle accelerates, F is larger for the cases in which the acceleration is larger (for the same value of the speed). For the case of constant speed ($F = F_r + F_a + F_p$), the larger the value of the constant speed the larger the value of F as it is seen in Figure 5, because F_a depends on the square of the speed (F_r and F_p do not depend on the speed). For the parts 2 and 3 of the driving cycle there are jumps in the values of F because the values of the inertial mass of the vehicle change (and are discontinuous) as the vehicle changes gears; however, there are no jumps for the case of constant speed because the inertial mass does not contribute to F. When the vehicle travels at constant speed at the end of the parts 2 and 3 of the driving cycle, the value of F is larger for part 3 because the constant speed (104.6074 km/hr) is larger than that for part 2 (86.6081 km/hr), therefore F_a is larger and consequently F will be larger for part 3 of the driving cycle. The values of F for parts 2 and 3 when the vehicle travels at constant speeds, 86.6081 and 104.6074 km/hr respectively, are the same as the values of F for the corresponding values of the speed for the

cases in which the vehicle travels at constant speed during all the trip at those two particular values of the speed. That is why the values of F of the parts 2 and 3 intersect the values of F for the case of the vehicle traveling at constant speed. For parts 2 and 3 of the driving cycle the term $m_i a$ is the largest for the smallest speeds, and for larger values of the speed the term Ma is the largest and for the largest speeds F_a is the largest, because it has a dependence of V square.
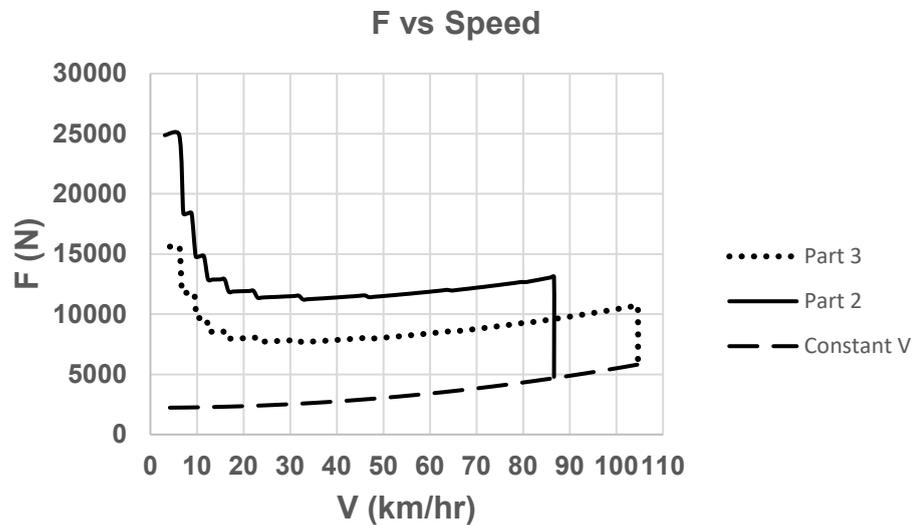

F vs Speed

Figure 5: Value of $F = F_r + F_a + F_p + Ma + m_i a$ versus speed for parts 2 and 3 of the driving cycle and for the case in which the speed is constant (for constant values of the speed from 4 up to 104.6074 Km/hr).

Figure 6 shows the engine torque, T_e, which is the torque that the engine provides for the vehicle to move and that it is equal to F times the radius of a wheel, r_w, divided by R_{eff}. For the same speed, R_{eff} is the same for the cases of the two parts of the driving cycle and the case of the vehicle moving at constant speed. Thus, for the same value of the speed, if F is larger for the two parts of the driving cycle than for the case of constant speed, T_e will be also larger for those two parts than for the case of constant speed. And if F is larger for the part 2 than for the part 3 of the driving cycle then T_e will be larger for the part 2. As it is noticed in Figure 6, T_e, has jumps because it is obtained by dividing F by R_{eff}; and R_{eff} is discontinouos as a function of the speed and its value is smaller for larger values of the speed. As T_e is obtained by multipying F by the radius of the wheel, r_w, the engine torque depends on that radius and therefore the fuel economy will also depend on the size of the wheel.
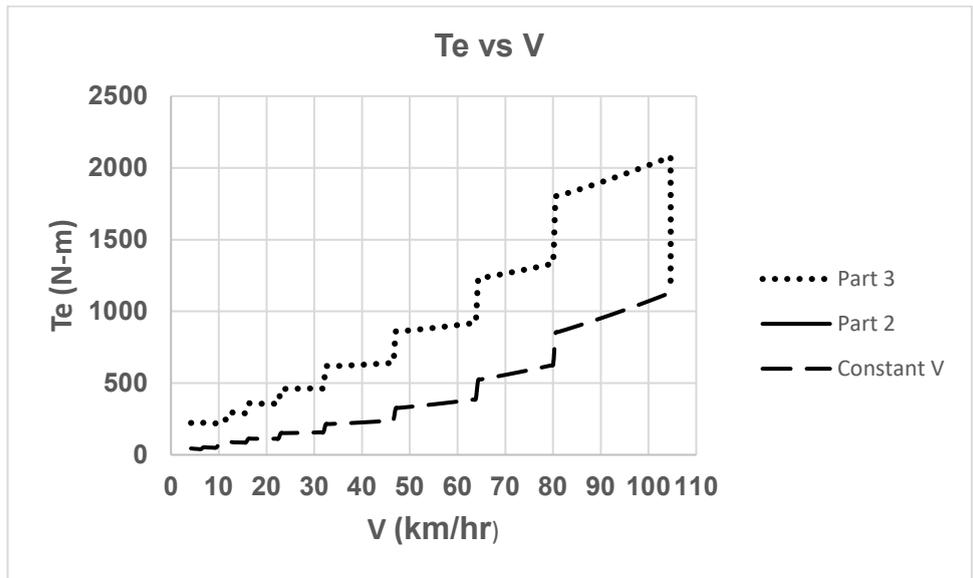
Figure 6: Engine torque, T_e, versus speed of the vehicle for parts 2 and 3 of the driving cycle and for the case in which the speed is constant (for constant values of the speed from 4 up to 104.6074 Km/hr).

The engine fuel consumption for a few pairs of rpm and T_e is shown in Figure 7. The values for the fuel consumption were taken directly from the first version of the GEM software developed by the US EPA. In the table of the US EPA there are 17 times 31 values of fuel consumption and then an interpolation is carried out to obtain the values of the fuel consumption for any value in the range of rpm from 600 up to 2200 and in the range of the torque from 0 up to 3000 N-m. The fuel consumption obtained by interpolation using the 31 times 17 table for rpm=1267.3064 and rpm=1498.0440 for several values of T_e are provided in Figure 7.
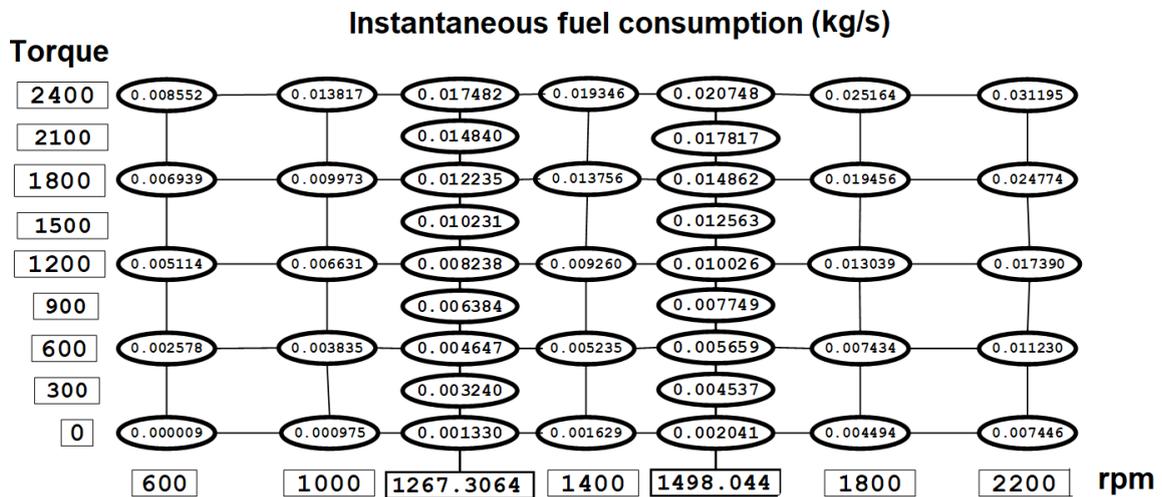

Figure 7: Instantaneous engine fuel consumption in kg/s for pairs of the engine torque and rpm.

Figure 8 shows the instaneous fuel consumption of the engine versus the speed of the vehicle. For the same rpm the instaneous fuel consumption increases as the engine torque increases, therefore for the same value of the speed (see Equation 7) the fuel consumption will be larger for larger values of the engine torque. Thus, for the same speed, the fuel consumption for the two parts of the driving cycle will be larger (because the engine torques are larger for them) than for the case of constant speed, as it can be seen in Figure 8. For the case of constant speed, as the torque is larger

for larger speeds, the fuel consumption will increase (in average) if the vehicle moves at larger speeds.
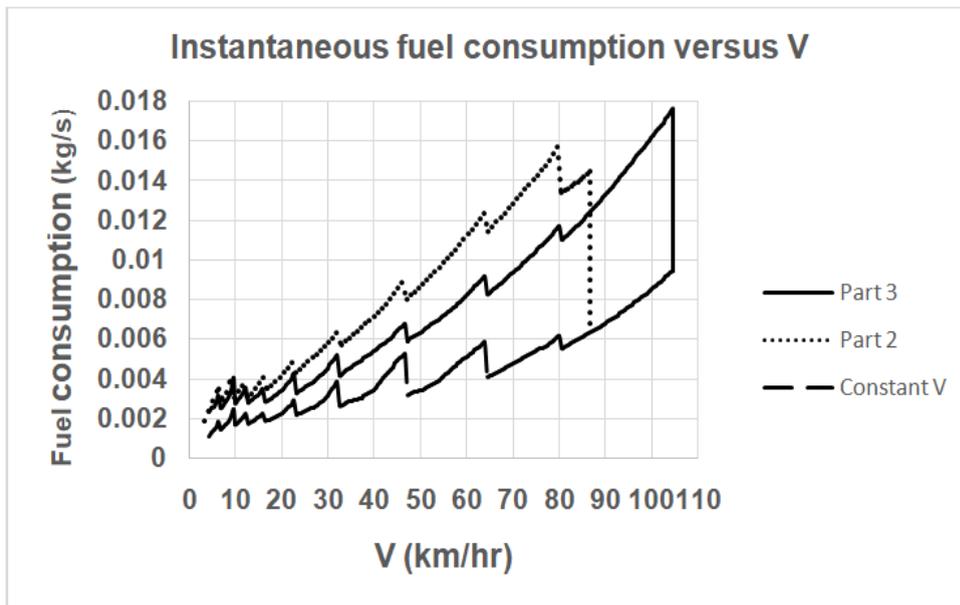
Figure 8: Instantaneous fuel consumption for parts 2 and 3 of the driving cycle and for the case in which the speed is constant (for constant values of the speed from 4 up to 104.6074 Km/hr), versus the speed of the vehicle.

Figure 9 shows the results for the fuel economy versus the speed of the vehicle for the parts 2 and 3 of the driving cycle and for the cases of constant speed (for constant values of the speed from 4 up to 104.6074 Km/hr). For speeds less than 35 km/hr, the fuel economy increases (in average) as the vehicle increases its speed with some sudden jumps when there is a change of gears in the case of the parts of the driving cycle in order to increase the speed of the vehicle, and when different gears are used for different values of the constant speed in the case in which the vehicle travels with constant speed during all the trip. The largest fuel economy is reached for the speed of 64.33 km/hr and it is of 3.71 km/liter; it is at this speed in which the vehicle travels at constant speed and therefore there is no acceleration of the vehicle and the needed torque to move the vehicle is smaller (see Equation 11). The fuel economy for the vehicle moving in the part 3 of the driving cycle is larger than for the case of part 2 because the acceleration in the part 3 of the driving cycle is smaller than for the part 2 (as it can be seen in Figure 1). The results of parts 2 and 3 show that the fuel economy depends on the acceleration of the vehicle and comparing these two cases, the conclusion is that when the acceleration is smaller the fuel economy is larger. The results of part 2 and 3 of the driving cycle show that after the vehicle stop accelerating, when the vehicle travels at constant speed the fuel economy increases appreciably and that the fuel efficiency for the case of part 2 of the driving cycle is larger than for the part 3 of the driving cycle. The last result is due to the fact that the final constant speed in the part 3 of the driving cycle (104.6074 km/hr) is larger than in the part 2 (86.6081 km/hr) and therefore F_a, the aerodynamic force is larger and then the needed torque to move the vehicle is larger which leads to a larger fuel consumption. When the vehicle reaches its highest speed (86.6081 km/hr in case of part 2 and 104.6074 km/hr in case of part 3 the vehicle travels in the 10th gear of the gearbox in both cases.
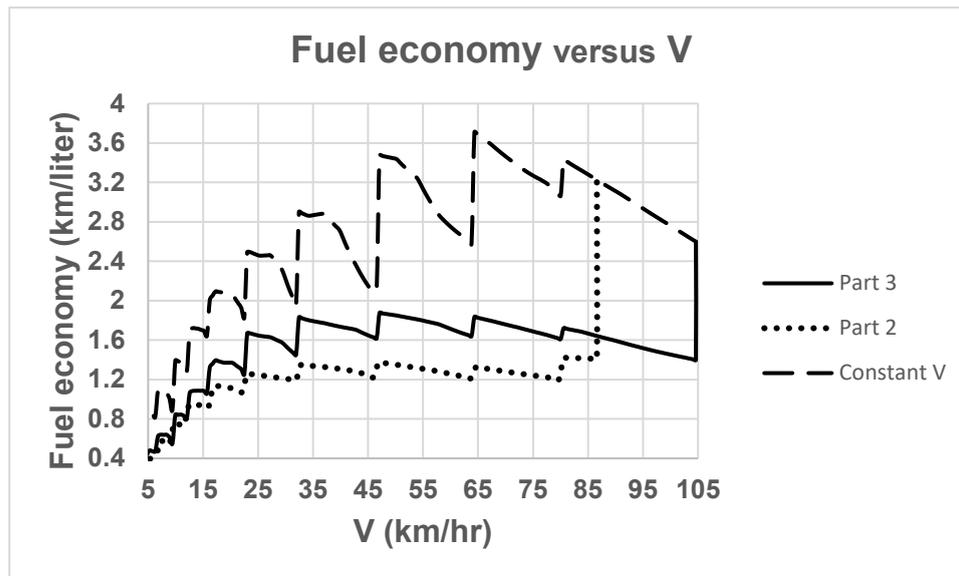
Figure 9: Fuel economy (km/liter) versus the speed of the vehicle for the 455 HP heavy duty vehicle moving in parts 2 and 3 of the driving cycle and for the cases of constant speed. Load 17236 kg.

The fuel economy has a maximum (as it is seen in Figure 9) even though the fuel consumption increases with the speed because is the ratio of the distance travelled (which increases with the speed) over the fuel consumption. Notice that when the speed is equal to 86.6081 km/hr the fuel economy of part 2 of the driving cycle and that of constant speed are the same (and equal to 3.22515102 km/liter) as it should be, because in both cases at that speed the vehicle is travelling at constant speed. Likewise, for the part 3 of the driving cycle and the case of constant speed at the speed of 104.6074 in which both have a fuel economy of 2.59914436 km/liter. Definitely travelling at constant speed increases the fuel economy and the best constant speed in this case is of 64.44 km/hr.

For a load of 17.236 tons and zero slope of the road, the results in Figures 6, 7 and 8 explain the fuel economy obtained in Figure 9.

For the part 2 of the cycle, UAMmero also provides the following results for the trip: 4.862631 liter of fuel consumed. 14.752320 km of distance travelled. 0.012643 tons of CO_2 emitted. 3.0338149 km/liter of fuel economy. 0.329618 liter/km. 0.019124 liter/(ton*km), the ton refers to the transported load. 49.721919 g/(ton*km) of CO_2, the ton refers to the transported load. 5.6372 dollars (at 1.1593 dollars/liter) of payment for fuel. 0.151714 US dollars for environmental damage (at 12 US dollars the ton de CO_2).

For part 3 of the driving cycle: 6.808530 liter of fuel consumed. 17.387621 km of distance travelled. 0.017702 tons of CO_2 emitted. 2.55380223 km/liter of fuel economy. 0.391573 liter/km. 0.022718 liter/(ton*km), the ton refers to the transported load. 59.067700 g/(ton*km) of CO_2, the ton refers to the transported load. 7.8931 dollars of payment for fuel. 0.212426 US dollars for environmental damage.

On the other hand, driving at a constant speed of 64.33 km/hr the fuel economy is of 3.71 km/liter. For a distance of 14.752320 km (the distance travelled in the part 2 of the driving cycle) the fuel consumption would be of 3.97636658 liters and the cost of the trip would be of only 4.6098 dollars (a saving of 18.225 %). There would be also a reduction of 18.225 % in the CO_2 emissions.

Driving at a constant speed of 64.33 km/hr, for a distance of 17.387621 km (the distance travelled in the part 3 of the driving cycle) the fuel consumption would be of 4.6866903 liters and the cost of the trip would be of only 5.4333 dollars (a saving of 31.1640 %). There would be also a reduction of 31.1640 % in the CO_2 emissions.

Therefore, the recommendation would be to maintain an appropriate constant speed when

travelling in highways; although it is necessary to accelerate to reach the constant speed.

4.2 200 HP heavy truck

For the 200 HP heavy truck several results are presented by changing the transported load as well as the slope of the road.

4.2.1 Results for the fuel economy for parts 2 and 3 of the driving cycle and for the case of constant speed (for constant values of the speed from 4 up to 104.6074 Km/hr) for 0° of inclination of the road

In Figure 10 the values of the fuel economy as a function of the speed are presented for a transported load of 2 tons, and 0° of inclination of the road, for the two parts of the driving cycle and the case of constant speed. As for the case of the 455 HP heavy duty vehicle the fuel economy is larger for the case in which the vehicle does not accelerate at any moment because it travels at constant speed. The maximum fuel economy is of 9.88171586 km/liter at the constant speed of 52.303608 km/hr. The fuel economy is better for the case of constant speed, as it was seen in the previous section, because the engine torque in that case is smaller than the corresponding engine torque for the two parts of the driving cycle (for the same speed of the vehicle) because the acceleration of the vehicle is zero. And the fuel economy for the part 3 of the driving cycle is larger than for the part 2 (for the interval of speeds in which the vehicle accelerates) because the acceleration of the vehicle is smaller in the part 3 of the cycle.

For the part 2 of the cycle, the following results are obatined: 2.648253 liter of fuel consumed. 14.752320 km of distance travelled. 0.006885 tons of CO_2 emitted. 5.57059617 km/liter of fuel economy. 0.179514 liter/km. 0.089757 liter/(ton*km), the ton refers to the transported load. 233.368657 g/(ton*km) of CO_2, the ton refers to the transported load. 3.0701 dollars of payment for fuel. 0.082625 US dollars for environmental damage.

For part 3 of the driving cycle: 3.931462 liter of fuel consumed. 17.387621 km of distance travelled. 0.010222 tons of CO_2 emitted. 4.42268484 km/liter of fuel economy. 0.226107 liter/km. 0.113053 liter/(ton*km), the ton refers to the transported load. 293.939057 g/(ton*km) of CO_2, the ton refers to the transported load. 4.5577 dollars of payment for fuel. 0.122662 US dollars for environmental damage.

On the other hand, driving at a constant speed of 52.303608 km/hr the fuel economy is of 9.88171586 km/liter. For a distance of 14.752320 km (the distance travelled in the part 2 of the driving cycle) the fuel consumption would be of 1.49289053 liters and the cost of the trip would be of only 1.7307 dollars (a saving of 43.6272 %). There would be also a reduction of 43.6272 % in the CO_2 emissions. Driving at a constant speed of of 52.303608 km/hr, for a distance of 17.387621 km (the distance travelled in the part 3 of the driving cycle) the fuel consumption would be of 1.75957508 liters and the cost of the trip would be of only 2.0399 dollars (a saving of 55.2428 %). There would be also a reduction of 55.2428 % in the CO_2 emissions. Therefore, the recommendation would be to maintain an appropriate constant speed when travelling in highways; although it is necessary to accelerate to reach the constant speed.
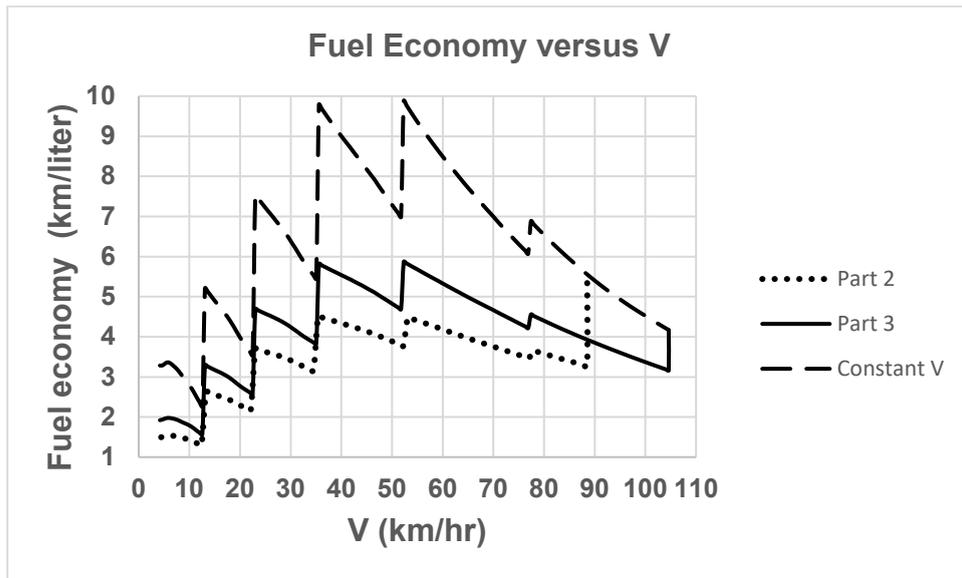
Dependence of Fuel Economy on Speed for Heavy Duty Vehicles

Fuel Economy versus V

Figure 10: Fuel economy (km/liter) for the two parts of the driving cycle and for constant speed (for constant values of the speed from 4 up to 104.6074 Km/hr) versus speed, for the 200 HP heavy truck, zero slope and 2 tons of load.

The next results in the rest of this section correspond to the vehicle moving with constant speed.

4.2.2 Constant speed, 0° degrees of inclination of the road and different values of the transported load

The results for the fuel economy versus the speed for the 200 HP heavy truck for constant speeds from 4 to 104.6074 km/hr for different values of

the transported load and zero slope are presented in Figure 11. In this case the value of F is given by Equation 11 for θ = 0° and the only term which depends on the load is $F_r = C_r Mg$, where M is the sum of the masses of the vehicle and the load. The increment of the load from 0.1 to 5 tons does not affects significantly the fuel economy of the vehicle for the values of the constant speeds considered.
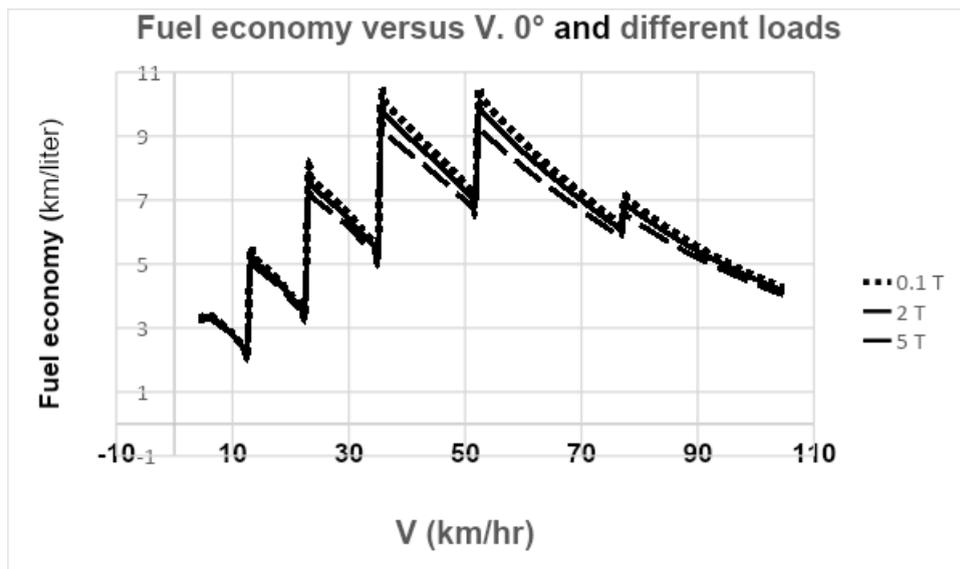
Fuel economy versus V. 0° and different loads

Figure 11: Fuel economy for the 200 HP heavy truck with different loads, zero slope and moving with constant speed (for constant values of the speed from 4 up to 104.6074 Km/hr). The masses of the loads are 0.1, 2 and 5 tons.

4.2.3 Constant speeds, 2 tons of transported load and different degrees of inclination of the road

The F_p force becomes the largest term in Equation 11 for some values of the inclination of the road. A large value of F_p results in a very large value of the necessary torque to move the vehicle that for some values of the speed results larger than $T_{e,\,max}$; therefore, even though the vehicle does not accelerate, the maximum constant speed at which the vehicle can move has a limit. The maximum value of the vehicle constant speed is that which results in a torque equal than the maximum torque that the engine can provide for that speed, as it is shown in Figure 12.

In Figure 12 are shown the values of the torque, versus the speed for the 200 HP heavy truck which transports 2 tons of load and which travels in roads with different inclinations. The maximum values of the torque that the engine can provide, $T_{e,max}$, versus the speed are also plotted. It can be noted that the maximum constant speed at which the vehicle can travel occurs when the engine torque, T_e, necessary to move the vehicle intersects the curve of $T_{e,max}$.
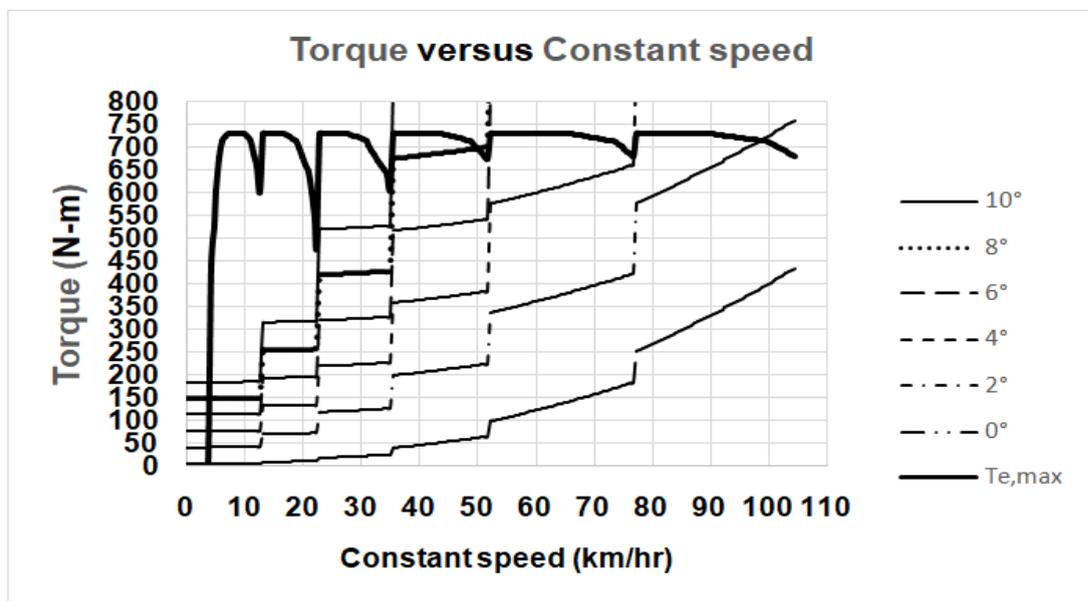

Figure 12: Maximum torque, $T_{e,max}$, and necessary torque, T_e, to move the 200 HP heavy truck with 2 tons of load in a road with different inclinations versus the constant speed of the vehicle.

The results for the fuel economy for the 200 HP heavy truck for a transported load of 2 tons and different values of the inclination of the road are presented in Figure 13. As the inclination angle of the road increases, the maximum constant speed in which the vehicle can move is smaller and the decrement in the values of the fuel economy is large. As it can be seen in Figure 13, travelling at constant speeds in a road with inclination of 10° results in a fuel efficiency around one tenth of the one reached when travelling at constant speed of 52.303608 km/hr in a road with 0°. This implies that the CO2 emissions in a trip in a road with an inclination of 10° will emit 10 times the CO_2 emissions than travelling in a road with 0° with a speed of 52.303608 km/hr. The trip in the steep road would be ten times more expensive than the trip in the flat road travelling at a speed of 52.303608 km/hr.
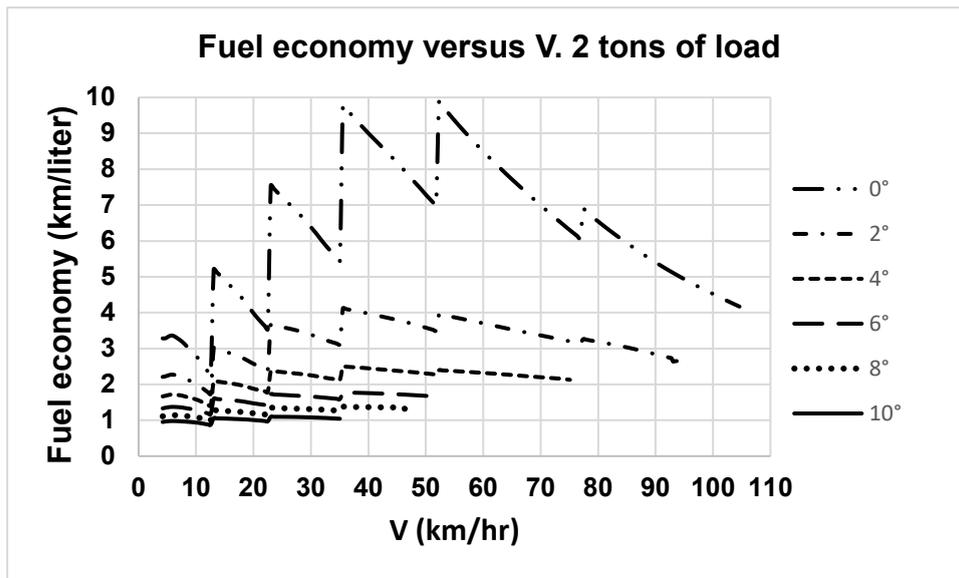
Fuel economy versus V. 2 tons of load

Figure 13: Fuel economy when the vehicle with two tons of load moves with constant speed on a road with different slopes

The recommendation of driving at constant speed can be done for driving in highways because in urban regions vehicles accelerate and deaccelerate constantly because of the traffic lights and many vehicles on the streets.

V. CONCLUSIONS

There are considerable savings in fossil fuels and an apreciable reduction of CO_2 emissions by driving at certain speeds and accelerations depending on the vehicle being driven, the engine, final drive, gearbox and wheels of the vehicle, the loads being transported and the slope of the roads. Driving at some constant speeds reduces the fuel consumption although those speeds are reached after accelerating the vehicle starting from a low speed. To maximize the savings, technical training of heavy-duty vehicle drivers is necessary. However, even drivers of passenger vehicles should be aware of the benefits of knowing that it is posible to save fuel if they consciously and purposely drive at the best speeds according to the routes they travel. In any case, the recommendation for any driver is: know your vehicle. Besides, the reduction in fuel and CO_2 emissions increase the energy security of the countries and the care of the global environment.

REFERENCES

1. EPA and NHTSA 2016 *Greenhouse Gas Emissions and Fuel Efficiency Standards for Medium and Heavy Duty Engines and Vehicles-Phase 2* (United States: Federal Register)
2. Zacharof NG and Fontaras G 2016 *Report on VECTO Technology Simulation Capabilities and Future Outlook* (Luxembourg: Publications Office of the European Union).
3. DN Dominguez-Perez, JL Pantoja-Gallegos and N Dominguez-Vergara 2021 Dynamics of a heavy-duty vehicle in a driving cycle *J. Phys. Conf. Ser.* **1723** 012035
4. J. Garcia-Osorio, A. Maldonado-Susano, N. Dominguez-Vergara, *Methods and results of training economically technical driving in Mexico*, EDULEARN 2019 Proceedings, pp. 7439-7448, 2019.
5. Environmental Protection Agency 2010 *Greenhouse Gas Emissions Model (GEM) User Guide* (United States: EPA).

London Journal Press Membership

London Journals Press membership is an elite community of scholars, researchers, scientists, professionals and institutions associated with all the major disciplines. London Journals Press memberships are for individuals, research institutions, and universities. Authors, subscribers, Editorial Board members, Advisory Board members, and organizations are all part of member network.

Read more and apply for membership here:
https://journalspress.com/journals/membership

For Authors

For Institutions

For Subscribers

Author Membership provide access to scientific innovation, next generation tools, access to conferences/seminars /symposiums/webinars, networking opportunities, and privileged benefits.
Authors may submit research manuscript or paper without being an existing member of LJP. Once a non-member author submits a research paper he/she becomes a part of "Provisional Author Membership".

Society flourish when two institutions come together." Organizations, research institutes, and universities can join LJP Subscription membership or privileged "Fellow Membership" membership facilitating researchers to publish their work with us, become peer reviewers and join us on Advisory Board.

Subscribe to distinguished STM (scientific, technical, and medical) publisher. Subscription membership is available for individuals universities and institutions (print & online). Subscribers can access journals from our libraries, published in different formats like Printed Hardcopy, Interactive PDFs, EPUBs, eBooks, indexable documents and the author managed dynamic live web page articles, LaTeX, PDFs etc.

GO GREEN AND HELP
SAVE THE ENVIRONMENT

JOURNAL AVAILABLE IN

PRINTED VERSION, INTERACTIVE PDFS, EPUBS, EBOOKS, INDEXABLE
DOCUMENTS AND THE AUTHOR MANAGED DYNAMIC LIVE WEB PAGE
ARTICLES, LATEX, PDFS, RESTRUCTURED TEXT, TEXTILE, HTML, DOCBOOK,
MEDIAWIKI MARKUP, TWIKI MARKUP, OPML, EMACS ORG-MODE & OTHER

SCAN TO KNOW MORE

support@journalspress.com
www.journalspress.com

*THIS JOURNAL SUPPORT AUGMENTED REALITY APPS AND SOFTWARES